[AMERICAN JOURNAL OF SCIENCE, VOL. 290, JUNE, 1990, P. 666–718]

MULTIVARIABLE PHASE DIAGRAMS: AN ALGORITHM BASED ON GENERALIZED THERMODYNAMICS

J. A. D. Connolly*
Department of Geosciences, The Pennsylvania State University, University Park, Pennsylvania 16802

ABSTRACT. There are only two basic types of phase diagram variables, *potentials* (for example, P, T, and μ_k), defined by the partial derivative of one extensive property with respect to another, and *compositions,* defined arbitrarily as a ratio of extensive properties (for example U, H, S, V, and n_k). Each variable has a different physicochemical significance, but from a computational perspective there is no reason to distinguish among the variables of each group. Recognition of this serves as a basis for a method of calculating and interpreting phase diagrams that is completely general with respect to the variables chosen for any problem. This method can be used to calculate some unusual diagrams (polythermal and polybaric projections), but the utility of such diagrams is obscured by the conventional notions of components and composition. The logical extension of these notions into the context of a general thermodynamic model requires that a *component* is associated with each independent conservative extensity of a system. For example, in the analysis of an isochoric or adiabatic system, it is necessary to include a component that determines the mechanical property (V) or thermal property (for example, H), respectively, of the system. The relative amounts of the components, defined in this general sense, are the thermodynamically significant *composition* of a system. The interpretation of such a composition is exactly analogous to the interpretation of the chemical composition for a chemically closed system. This understanding of components and composition emphasizes the underlying canonical basis of thermodynamics and reveals basic similarities in the analysis of all physicochemical models.

By incorporating generalized concepts, the mechanics of phase diagram calculations for multivariable systems have been reduced to a simple algorithm which has been automated with a computer program called Vertex. Vertex is based on an abbreviated combinatorial algorithm which derives a piecewise linear approximation of the isopotential thermodynamic surface for a system. This approximation is accomplished by modeling the continuous nonlinear thermodynamic surfaces of solution phases by inscribed polyhedra, the vertices of which are considered to define *pseudocompounds.* Because the approximated thermodynamic surface of the system is piecewise linear, changes in its geometry or topology are easily detected as one potential is varied to define low variance phase equilibria. Low variance equilibria can then be traced as a function of a second potential. Computations can be terminated at different levels in this sequence to obtain a composition, mixed-variable, or Schreinemakers

* Current address: Institute für Mineralogie und Petrographie, ETH-Zentrum, CH-8092 Zürich, Switzerland

diagram. It is also possible to trace low variance equilibria between pseudocompounds representing the same phase. The conditions of such equilibria define an isoplethal contour of a high variance phase field, and these contours can be shown in Schreinemakers diagrams to characterize high variance equilibria. The strategy of Vertex minimizes the combinatorial aspect of phase diagram calculations; it is thus well suited for problems in which the stable phase equilibria cannot be prescribed and all possible equilibria must be considered simultaneously. In addition to potentials and compositions, the computational variables for Vertex may include related variables such as the composition or activity of a saturated phase (for example, a fluid). A variety of buffering and sectioning constraints can also be imposed within Vertex to simplify the phase diagrams of complex systems.

INTRODUCTION

The topologies and calibrations of phase diagrams are of great importance to petrologists. Since the work of Schreinemakers (1965[1]) and Roozeboom (1904), much attention has been focused on the topologic constraints of phase diagrams. This avenue of investigation is of value because it allows theoretically rigorous, though qualitative, integration and extension of knowledge from a variety of sources. The need for this qualitative approach stemmed from uncertainty in the thermodynamic parameters of phases of geologic interest. However, considerable effort has been made toward obtaining thermodynamic data for rock forming minerals (Robie and Waldaum, 1968; Nuamov, Ryzhenko, and Khoclakovsky, 1971; Helgeson and others, 1978; Robie, Hemingway, and Fisher, 1978; Haas, Robinson, and Hemingway, 1981; Robinson and others, 1983; Holland and Powell, 1985; Berman, 1988; et cetera), so that direct quantitative calculation of phase diagrams is now possible. Although these calculations are simple in concept, they involve such a large number of operations that they must be automated to be practical on an ab initio basis, even for relatively simple chemical systems. This paper, which describes a strategy for the automated construction of phase diagrams from thermodynamic equations of state, presents an attempt to fulfill this need.

This paper consists of two parts: in the first part certain aspects of canonical thermodynamic formalism are presented, and in the second part the application of this formalism in an algorithm and computer program for the construction of multivariable phase diagrams is discussed. The objectives in developing this program were to design an efficient and completely automated procedure which (1) would be general with respect to the choice of independent variables, (2) would not require assumptions about phase stabilities and compatibilities, and

[1] The work of F. A. H. Schreinemakers, which extended Roozeboom's (1904) treatise, was published as a series of forty-seven articles appearing in the *Proceedings of Koninkliijke Akadamie van Wetenshapen Te Amsterdam,* between 1898 and 1915. Reference is made here to a collection of these papers published and preserved by The Pennsylvania State University.

(3) would be independent of the form of analytic expressions for the energy of solution phases as a function of composition.

The conventional framework for the interpretation of phase diagrams is based largely on Gibbs' (1957[2] p. 63) notion of components applied to isobaric-isothermal chemically closed systems. In this context, components are defined as the smallest set of chemical entities necessary to specify the chemical composition of all possible phases of a system. This definition has special utility for an isochemical system because the components of such a system correspond to its independent extensive properties. However, because the isochemical system is a special case of a more general thermodynamic model, the conventional notion of components is unwieldy when applied to adiabatic, isochoric, or chemically open systems. Recognition of this in petrology has led to the distinction between "mobile" and "inert" components for chemically open isobaric-isothermal systems (Korzhinskii, 1959; Thompson, 1954). For such systems, the chemical potentials of "mobile" components are variable properties analogous to pressure and temperature, and the "inert" components have a role identical to the components of a chemically closed isobaric-isothermal system. The success of this approach reflects the fact that the components of a chemically open system are a subset of those of a chemically closed system. However, the utility of Korzhinskii's "mobile" and "inert" components fails for adiabatic or isochoric systems because these systems have thermal or mechanical extensive properties which cannot be described by chemical components. The intent of Part I of this paper is to avoid this shortcoming by extending the idea of thermodynamic components and composition into the context of a general thermodynamic model. When components are understood in this context, it becomes relatively simple to understand the phase relations of adiabatic and isochoric systems in light of conventional techniques. More importantly, with reference to computational methods, thermodynamic generalization demonstrates that identical logic can be applied to the calculation and interpretation of any phase diagram, regardless of the variables under consideration.

The presentation of generalized thermodynamics in Part I is used as the basis for the explanation of the computational strategy for construction of multivariable phase diagrams in Part II. Although generalized thermodynamics is useful in the interpretation of phase diagrams, and essential for the development of efficient computational methods, an understanding of generalized thermodynamics is unnecessary for the application of such methods for most petrologic problems.

[2] J. Willard Gibbs established the theory of phase equilibria and chemical thermodynamics in a series of articles that appeared between 1873 and 1878 in the *Transactions of the Connecticut Academy*. These papers were subsequently published as *The Scientific Works of J. Willard Gibbs* in 1906 and later as the more complete publication *The Collected Works of J. Willard Gibbs* in 1928, 1948, and 1957. Reference is made here to the third printing of this last publication.

For this reason, an attempt has been made to make Parts I and II as independent as possible.

A computer algorithm and program, Bounds, for calculating composition phase diagrams was described by the author in a previous paper (Connolly and Kerrick, 1987). Connolly and Kerrick also discussed the use of Bounds within a more comprehensive algorithm for constructing phase diagrams as a function of other variables. This comprehensive algorithm was implemented earlier (Connolly and Kerrick, 1984) but has now been discarded in favor of the algorithm discussed here in Part II. Bounds cannot be used to calculate phase diagrams as a function of variables like pressure and temperature, but its algorithm is still the basis of the methods described in Part II.

PHASE DIAGRAM NOMENCLATURE

The independent variables of phase diagrams can be related to a simple ratio of extensive properties (for example, chemical composition) or to an intensive state function (for example, P, T, $\mu_1, \ldots, \mu_k$). Both kinds of variables are intensive, and to distinguish them they will be designated *compositional* (Hillert, 1985a; Palatnik and Landau, 1964) and *potential* variables, respectively. It is convenient to consider these variables to be the representative coordinates of a *system* and its constituent phases. The association of the variables of a diagram with the determinative physicochemical properties of a real system is, of course, unspecified because it is impossible to prescribe the way a phase diagram will be used.

A diagram is considered to be a *phase diagram* only if its geometry defines the respresentative coordinates of both a system and the stable equilibrium phases of the system (Schmalzried and Pelton, 1973; Lukas, Weiss, and Henig, 1982; Hillert, 1985a). For multicomponent systems there are two basic kinds of phase diagrams, *composition diagrams* that show phase relations only as a function of composition, and *mixed-variable* diagrams that show phase relations as a function of both potentials and composition. Phase diagrams are composed of geometric elements or *phase fields* that define the loci of conditions for which a specific phase assemblage is in equilibrium. The term phase field is used to describe an element of any dimensionality (Hillert, 1985a), whereas the term *phase region* is applied only to geometric elements of the same dimension as the corresponding diagram. In discussing phase diagrams it is useful to define the *variance* of a phase field, or equilibrium, of p phases as n − p, where n is equal to the number of components plus the number of independent potential variables for a diagram, that is, n − 1 is the dimension of the diagram.

The equilibrium phase relations of a system with more than two independent variables can be described by a multidimensional phase diagram. In general the information in such diagrams must be presented in two dimensions by sectioning or projection to be of value. Phase diagram sections may be defined by potential or composition sectioning

variables and are designated *potential* and *composition sections,* respectively. A variety of projection schemes has been proposed for the graphical representation of multidimensional phase diagrams (Palatnik and Landau, 1964); however, affine projections after Schreinemakers (1965; Korzhinskii, 1959; Zen 1966a, b) have proven the most effective. With the *Schreinemakers method,* univariant phase fields are projected onto a two-dimensional coordinate frame defined by two potentials. This scheme is based on the fact that univariant fields project as curves and that the intersections of these curves define conditions of invariant equilibria (invariant points). The term phase diagram is often incorrectly applied to composition sections and Schreinemakers projections. This usage is incorrect because neither of these diagrams defines the equilibrium phase compositions; in addition, Schreinemakers projections do not define high variance ($p < n - 1$) phase fields.

A physicochemical system is *open* with respect to some extensity if the extensity can be transferred to or from the systems environment. A system that is not open with respect to some extensity is *closed* with respect to that extensity. For brevity it is useful to describe a system by specifying only those properties to which it is open; closure with respect to all the unspecified properties. Thus, if a system is described as isochemical or chemically closed, the open character of this system with respect to volume and entropy is implicit. As phase diagrams show only equilibrium states, with reference to phase diagram systems the isobaric-isothermal nature of a chemically closed system is also implicit.

FREQUENTLY USED SYMBOLS

c —number of unconstrained components
k —number of fundamental kinds of matter
G —Gibbs free energy
H —enthalpy
n_k —number of moles of the k^{th} kind of matter
n —c plus the number of independent potentials
p —number of equilibrium phases
P —pressure
q —number of internally buffered components
S —entropy
T —temperature
U —internal energy
V —volume
X_j —composition of a system or phase with respect to the j^{th} unconstrained component
Y_j —composition of a system or phase with respect to the j^{th} component
α_i —reaction coefficient for the i^{th} phase
θ —potential state function
λ —thermodynamic component for adiabatic systems

μ_j —chemical potential of the j^{th} component
π —total number of phases considered to be possibly stable at the outset of a calculation
σ —number of endmember compositions of a solution phase
ϕ_i —composition vector for the i^{th} phase
ψ —extensive state function
Ω —dependent extensive state function in eq (1) usually "free energy" function
$\rightarrow$ —superscript indicating a matrix or vector quantity
$\wedge$ —superscript indicating a unit quantity of the superscripted property

PHASE NOTATION

Symbol	Phase	Chemical composition
Ab	albite	$NaAlSi_3O_8$
Ab_x	subcritical Ab-rich feldspar	Ab_xOR_{1-x}
AC_3	tricalcium aluminate	$Ca_3Al_2O_6$
Ad	andradite	$Ca_3Fe_2SI_3O_{12}$
An	anorthite	$CaAl_2Si_2O_8$
And	andalusite	Al_2SiO_5
CA	calcium aluminate	$CaAl_2O_4$
C_2A	calcium dialuminate	$CaAl_4O_7$
C_6A	calcium hexaluminate	$CaAl_{12}O_{19}$
Cc	calcite	$CaCO_3$
Co	corundum	Al_2O_3
Cr	cristoballite	SiO_2
Ep-cpd	epidote compound	$Ca_2FeAl_2Si_3O_{12}(OH)$
Fs	ferrosillite	$FeSiO_3$
Ge	gehlenite	$Ca_2Al_2SiO_7$
Gr	grossularite	$Ca_3Al_2Si_3O_{12}$
Gr_x or Gt	garnet solution	Gr_xAd_{1-x}
Hm	hematite	Fe_2O_3
Ky	kyanite	Al_2SiO_5
La	larnite	Ca_2SiO_4
Lm	lime	CaO
Mu	muscovite	$KAl_3Si_3O_{10}(OH)_2$
Mu_x	subcritical Mu-rich mica	Mu_xPa_{1-x}
Pa_x	subcritical Pa-rich mica	Pa_xMu_{1-x}
Or	orthoclase	$KAlSi_3O_8$
Or_x	subcritical Or-rich feldspar	Or_xAb_{1-x}
Pa	paragonite	$NaAl_3Si_3O_{10}(OH)_2$
Pa_x	subcritical Pa-rich mica	Pa_xMu_{1-x}
Pw	pseudowollastonite	$CaSiO_3$
Q	quartz	SiO_2
Rn	rankinite	$Ca_3Si_2O_7$
S	silica melt	SiO_2
Sil	sillimanite	Al_2SiO_5

S_xA_y	CAS melt	$(CaO)_{1-x-y}(Al_2O_3)_y(SiO_2)_x$
SC_3	tricalcium silicate	Ca_3SiO_5
Tr	tridymite	SiO_2
Wo	wollastonite	$CaSiO_3$
Zo	zoisite	$Ca_2Al_3Si_3O_{12}(OH)_2$
Zo_x or Ep	epidote solution	$Zo_x(Ep\text{-}cpd)_{1-x}$

PART I. THERMODYNAMIC GENERALIZATION

There are three basic types of thermodynamic properties: extensive properties (for example U, S, V, $n_1, \ldots, n_k$), potentials, defined by the partial derivative of one extensive property with respect to another, and compositions, defined as a ratio of extensive quantities. This definition of composition is somewhat broader than conventional usage, and its use will be justified later. Although each variable has a different physicochemical significance, from a computational perspective there is no reason to distinguish among the variables within each group. Consequently, it is possible to develop computer methods for calculating phase diagrams that are completely general with respect to the variables specified for any problem. These computer methods can perform a much wider variety of calculations than currently in use, and the question naturally arises as to which calculation is optimal for a particular problem. A broad thermodynamic formalism, though perhaps initially difficult to grasp, not only makes the applicability of such calculations apparent, but also demonstrates that seemingly exotic calculations require only minor modification of well known principles. In the following sections certain aspects of this formalism and the notions of thermodynamic composition and components are introduced. The reader may wish to refer to Hillert (1985a) for an excellent review on the generalization of phase diagrams and to Tisza (1966), Buchdahl (1966), and Rey de Luna and Zamora (1986a, b) for theoretical justification and amplification of this discussion.

THERMODYNAMIC COMPONENTS

A thermodynamic system is characterized uniquely by the values of a set of n + 1 extensive macroscopic properties (Gibbs 1957 p. 63). In general, it is supposed that more than one thermodynamic state is consistent with any given material configuration of a system, where a material configuration is defined by the relative amounts of each extensive property. It follows that one coordinate is required to differentiate the states of the system, and remaining n properties specify the material configuration of the system. If a spontaneous change of state is possible in such a system, then this former property must be nonconservative and capable of variations independent of the other n properties. Properties of this kind, such as entropy, are *nondeformation* properties, and all other properties are *deformation* properties (Born, 1964, p. 143; Landsberg, 1956; Buchdahl, 1966 p. 9; Gokcen, 1975, p. 107).

Variation in the state[3] and extent of an equilibrium system can be described by the relation:

$$d\Omega = \sum_{j=1}^{c} \theta_j \, d\psi_j - \sum_{j=c+1}^{n} \psi_j \, d\theta_j , \tag{1}$$

where Ω is a generalized state function, and ψ_j and θ_j represent, respectively, the extensities and potentials of the system. Each dependent potential is related to its extensive conjugate by:

$$\theta_j = \left(\frac{\partial \Omega}{\partial \psi_j}\right)_{\psi_{i,i\neq j,i\leq c},\theta_{i,c<i\leq n}} \qquad (j = 1, \ldots, c), \tag{2}$$

and each dependent extensive property is related to its conjugate potential by:

$$\psi_j = \left(\frac{\partial \Omega}{\partial \theta_j}\right)_{\psi_{i,1\leq i\leq c},\theta_{i,i\neq j,c<i\leq n}} \qquad (j = c + 1, \ldots, n), \tag{3}$$

Ω can usually be interpreted as an extremal work function (Salamon, Anderson, and Berry, 1977) (for example Gibbs and Helmholtz free energy functions) and for the sake of generality will be referred to here as a *free energy* function. For a system subject to the constraints $\{0 = d\psi_1 = \ldots = d\psi_c = d\theta_{c+1} = \ldots = d\theta_n\}$, it will be supposed that Ω is formulated in such a way that the condition:

$$d\Omega \geq 0 \tag{4}$$

is true for all possible variations from a stable equilibrium. Condition (4) is therefore a necessary and sufficient criterion for stable equilibrium. If condition (4) is to provide an efficient criterion for stability, then Ω must also be a nondeformation property (Connolly, ms, app. B). A potential is undefined for a system unless it is uniform in all parts of the system.[4] Therefore specification of the constraints $\{0 = d\theta_{c+1} = \ldots = d\theta_n\}$ presupposes uniformity of the potentials $\{\theta_{c+1}, \ldots, \theta_n\}$. For heterogeneous systems it is convenient to express condition (4) as:

$$\sum_{i=1}^{p} d\Omega^i \geq 0, \tag{5}$$

[3] It is often written that the extent of a system is determined by its state, this is a matter of definition; the distinction between state and extent is maintained here following the usage of Gibbs (1957, p. 88). It may be noted that the relative extent of the different phases of a system can be completely specified by intensities.

[4] This statement must be modified for the special case that occurs when the conjugate extensive property of a potential is not a possible attribute in all parts of a system. In such cases the potential is nil where its extensive conjugate is absent, and its value in the other parts of the system is taken to be characteristic of the system in its entirety (Gibbs, 1957, p. 67, 68, 79).

where i indexes the phases of the system. It is easily demonstrated from eq (1) and condition (4) that in a heterogeneous system consisting of p coexistent phases the equalities:

$$\theta_j^1 = \ldots = \theta_j^P \qquad (j = 1, \ldots, c) \tag{6}$$

are necessary conditions for stable equilibrium.

In phase equilibrium, the problem is to characterize the p stable equilibrium phases of a system given the parameters $\{\psi_1, \ldots, \psi_c, \theta_{c+1}, \ldots, \theta_n\}$ for the system and the state functions $(\Omega^i, i = 1, \ldots, \pi)$ for each possible phase. The equilibrium phases are completely characterized by the parameters $\{\psi_1^i, \ldots, \psi_c^i, \theta_{c+1}^i, \ldots, \theta_n^i, (i = 1, \ldots, p)\}$. Because of the uniformity of potentials at equilibrium the paramters $\{\theta_{c+1}^i, \ldots, \theta_n^i, (i = 1, \ldots, p)\}$ are degenerate with the independent potentials of the given system as specified at the outset of a calculation. Consequently, the state of a system and its constituent phases can be defined by representative coordinates in a c-dimensional metric space which represents the quantities $\{\psi_1, \ldots, \psi_c\}$. Any coordinate in this space can be expressed as the sum of c vector components, $\{(\psi_1, 0, \ldots, 0), \ldots, (0, \ldots, 0, \psi_c)\}$. In thermodynamics, the "components" of a chemically closed system are taken as the extensive properties represented by such vector components, rather than the vector components themselves. Following this usage, *thermodynamic components* are defined here as the properties $\{\psi_1, \ldots, \psi_c\}$.

Although components are defined here on a computational basis, the choice of components, and the appropriate dependent state function in eq (1), is usually dictated by the physicochemical model for the system of interest. This follows by noting that the constraints $\{0 = d\theta_{c+1} = \ldots, d\theta_n\}$ can be maintained in a dynamic system only if the system is open with respect to $\{\psi_{c+1}, \ldots, \psi_n\}$ and the potentials $\{\theta_{c+1}, \ldots, \theta_n\}$ are determined by environmental conditions. Likewise the constraints $\{0 = d\psi_1 = \ldots = d\psi_c\}$ imply the system is closed with respect to the components $\{\psi_1, \ldots, \psi_c\}$, which are invariant for all internal processes.

To clarify the idea of components, as defined here, it may be useful to consider two possible models for the system CaO–SiO_2. For a chemically closed system the suitable independent variables in eq (1) are those of the Gibbs free energy $\{-P, T, n_{SiO_2}, n_{CaO}\}$:

$$dG = VdP - SdT + \mu_{SiO_2}\, dn_{SiO_2} + \mu_{CaO}\, dn_{CaO}. \tag{7}$$

If instead, the system is isochoric, closed with respect to CaO and open with respect to SiO_2, the appropriate state function, Ω, with the independent parameters $\{V, T, \mu_{SiO_2}, n_{CaO}\}$, can be obtained from eq (7) by the Legendre transformation:

$$\begin{aligned} d\Omega &= d(G - VP - \mu_{SiO_2}\, n_{SiO_2}) \\ &= -PdV - SdT - n_{SiO_2}\, d\mu_{SiO_2} + \mu_{CaO}\, dn_{CaO}. \end{aligned} \tag{8}$$

In a petrologic context, eq (7) is applicable to a system with P and T as environmentally determined properties and n_{SiO_2} and n_{CaO} as conservative properties, whereas eq (8) is appropriate when T and μ_{SiO_2} are environmentally determined and V and n_{CaO} are conservative properties. In these examples, both systems are two-component systems; for the isochemical system the components are $\{n_{SiO_2}, n_{CaO}\}$, and for the isochoric system the components are $\{V, n_{CaO}\}$.

The recognition that the conventional notion of components should be modified for physicochemical models other than isochemical systems is not unique to this work. For instance, Korzhinskii (1959) distinguishes the roles of SiO_2 in eqs (7) and (8) by designating SiO_2 an "inert component" in the former equation and a "perfectly mobile component" in the latter. "Inert components" are equivalent to the components of chemically open and closed systems as defined here. However, because "inert components" are defined as a subset of isochemical system components this treatment precludes the selection of properties such as volume and entropy as "inert components." Korzhinskii's treatment therefore becomes awkward when applied to isochoric or adiabatic systems. In contrast, the present approach emphasizes that the volume property of an isochoric system is in every way analogous to the chemical components of an isochemical system.

Thermal Components

Conservation constraints on nonthermal extensities $(V, n_1, \ldots, n_k)$ can be imposed independently of any other thermodynamic restrictions. For a given diathermal system, the nonthermal components are invariant coordinates for all environmental conditions, that is, all possible values of the independent potentials $\{\theta_{c+1}, \ldots, \theta_n\}$. This invariance is not a requisite for components as defined here, but it is useful if a phase diagram represents the variation of the potenitals $\{\theta_{c+1}, \ldots, \theta_n\}$. By definition, the properties of an adiabatic system must satisfy the relation:

$$0 = dU - \sum_{j=c+1}^{n} \theta_j \, d\psi_j \tag{9}$$

for all reversible variations of the properties $\{\psi_{c+1}, \ldots, \psi_n\}$, subject to the constraint $\{0 = d\psi_2 = \ldots = d\psi_c\}$. From eq (9) it follows that at constant $\{\theta_{c+1}, \ldots, \theta_n\}$ the property:

$$\lambda \equiv U - \sum_{j=c+1}^{n} \psi_j \, \theta_j \tag{10}$$

is conservative and a component in the context of the phase equilibrium problem as discussed earlier. Unfortunately, because $\lambda = f(\theta_{c+1}, \ldots, \theta_n)$, λ does not provide the basis for a useful coordinate in phase diagrams as

a function of the potentials $\{\theta_{c+1}, \ldots, \theta_n\}$. Inasmuch as phase diagrams represent equilibrium states, for which:

$$dS = d\lambda/T, \tag{11}$$

this difficulty can be circumvented by choosing the entropy of an adiabatic system as a component. This choice implies the identities $\psi_1 = S$, and $\Omega = \lambda$. In this regard it is important to recognize that λ is a deformation coordinate (Buchdahl, 1966) and therefore condition (2) describes variations to virtual, rather than actual, adiabatic states (Tisza, 1966; Connolly, ms, app. B).

THERMODYNAMIC COMPOSITION

In the analysis of phase relations, the absolute extent of a system and its phases are not ascribed significance. The extensive quantities in eq (1) can therefore be replaced by the relative proportions of the extensive quantities. In the most general sense, these proportions express the composition of matter with regard to its thermal, mechanical, and chemical state. However, for thermodynamic systems in which the parameters $\{\theta_{c+1}, \ldots, \theta_n\}$ are independent, only the relative proportions of the components of the system are determinative, and, in this sense, it is useful to include only these proportions in the definition of composition.

Because only $c - 1$ independent ratios can be formed among the properties $\{\psi_1, \ldots, \psi_c\}$, the most rational means by which these properties can be transformed into intensive quantities is by the transformation (Gibbs, 1957, p. 88, 115):

$$Y_j = \psi_j/\psi_c \qquad (j = 1, \ldots, c - 1), \tag{12}$$

where the quantities $\{Y_1, \ldots, Y_{c-1}\}$ are compositional parameters. This transformation is concise because c extensities are transformed into $c - 1$ compositions. It can also be demonstrated by application of the Gibbs-Duhem relation that for two equilibrium phases, if $Y_j^1 > Y_j^2$, then $\theta_j^1 > \theta_j^2$. This is of value if phase diagrams are constructed with compositional variables on more than one axis as emphasized by Hillert (1985a).

Although the compositional parameters $\{Y_1, \ldots, Y_{c-1}\}$ as defined by eq (12) have useful theoretical attributes, they have certain properties that are undesirable for numerical applications. These properties are a consequence of the fact that $\{Y_1, \ldots, Y_{c-1}\}$ define an unconfined space, and therefore a one-component phase may have an infinite coordinate. This destabilizes numerical computations and complicates the graphical analysis of composition. These complications are avoided here by the

adoption of the following transformation which is symmetrical with respect to the components:

$$Y_j = \frac{\psi_j}{\sum_{i=1}^{c} (\psi_i/\hat{\psi}_i)} \quad (j = 1, \ldots, c). \tag{13}$$

Where $\{\hat{\psi}_1, \ldots, \hat{\psi}_c\}$ represent unit quantities of the components, and the compositional parameters are subject to the constraint:

$$\sum_{j=1}^{c} (Y_j/\hat{\psi}_j) = 1. \tag{14}$$

Although there are no other theoretical constraints on compositions, for reasons of practical necessity, the composition space of any system considered here must be finite. For any real system a finite space may always be defined by selecting components such that $\{0 \leq Y_j \leq 1\}$ for any allowed composition. With this constraint the composition space of a system is restricted to a $c - 1$ dimensional simplex, the triangular ($c = 3$), and tetrahedral ($c = 4$), representations of which are familiar to petrologists. This transformation maintains a one-to-one correspondence between the compositions $\{Y_1, \ldots, Y_c\}$ and the extensive quantities $\{\psi_1, \ldots, \psi_c\}$ and is the mathematical equivalent of the normalization contraint used by Gibbs (1957, p. 119) in his analysis of isochemical systems.

Each kind of thermodynamic model system is described by a different set of components. Thus, a different composition space and free energy function is best suited for each model. The Ω-Y spaces appropriate for models other than isochemical systems are probably unfamiliar, but the principles for the analysis of Ω-Y space are identical to those employed in the analysis of G-Y space for isochemical systems. This identity is illustrated geometrically in figure 1 for the two models of the $CaO–SiO_2$ system discussed earlier with reference to eqs (7) and (8). For the isochemical system the independent compositional parameter is:

$$Y_{CaO} = \frac{n_{CaO}}{n_{CaO}/\hat{n}_{CaO} + n_{SiO_2}/\hat{n}_{SiO_2}}. \tag{15}$$

Assuming each phase is stoichiometric , that is, a compound, then the G-Y state of each phase can be represented by a point at constant {P, T} (fig. 1A). For the model that is isochoric and closed with respect to CaO, the independent compositional parameter is:

$$Y_{CaO} = \frac{n_{CaO}}{n_{CaO}/\hat{n}_{CaO} + V/\hat{V}}. \tag{16}$$

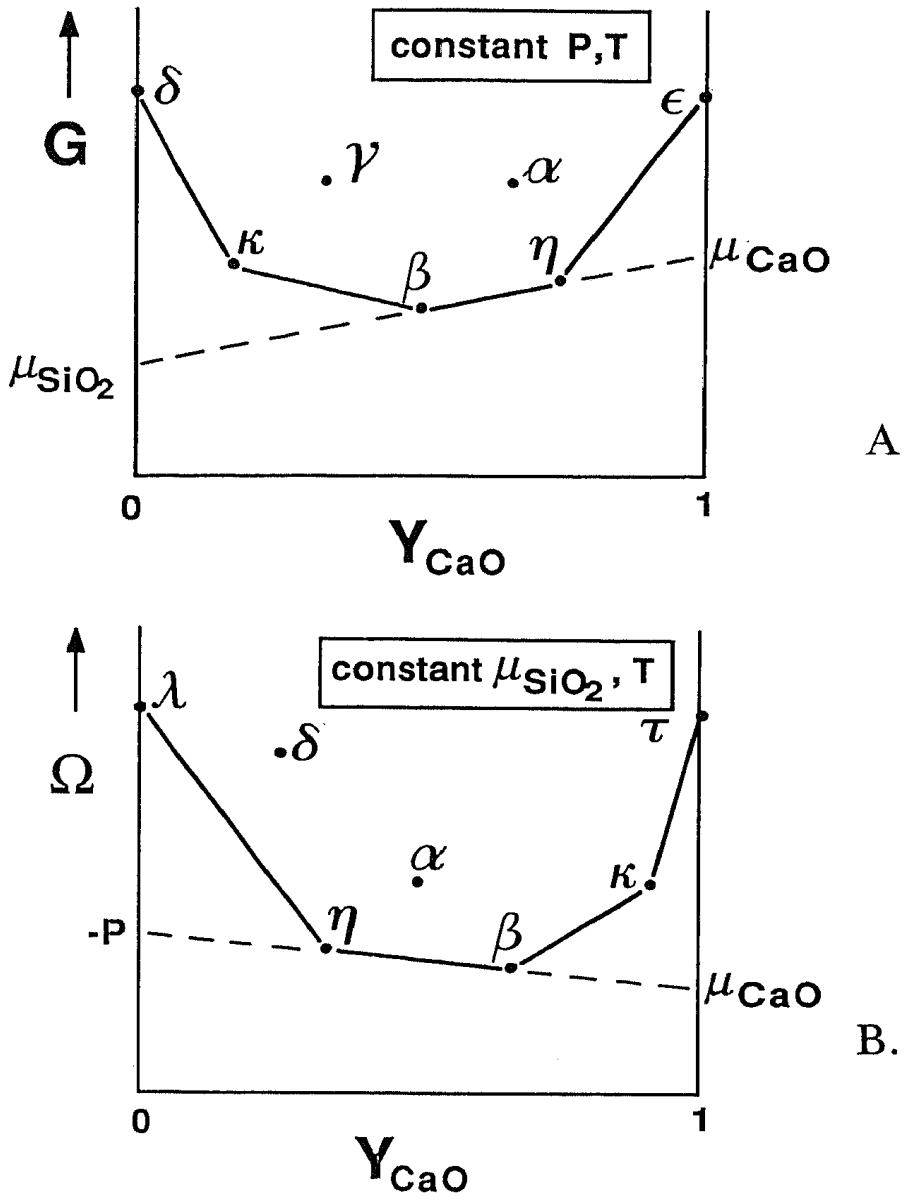

Fig. 1. Schematic free energy-composition diagrams for the system $CaO–SiO_2$. (A) G-Y diagram appropriate for the analysis of the isochemical system. (B) Ω-Y diagram appropriate for the analysis of the isochoric system closed with respect to CaO. The hypothetical phases indicated by greek letters are assumed to have fixed stoichiometry and molar volume. Note that (imaginary) phases τ and λ have infinite and zero density, respectively.

This parameter is closely related to density; thus, the Ω-Y state of a phase with constant molar volume (a common assumption for condensed phases) will be represented by a point in figure 1B at constant $\{\mu_{SiO_2}, T\}$. The compositional coordinates of a phase vary depending on the choice of components. Therefore, two phases compositionally equivalent in the composition space suitable for an isochemical system may become nondegenerate in the composition space suitable for an isochoric system. A similar effect is illustrated schematically by the phase δ which

is a one-component phase in the context of figure 1A and is a two-component phase in the context of figure 1B.

The stable state of a system with fixed composition will be defined by the phase assemblage of minimum free energy (condition 5). Given that the amount of a phase cannot be negative, it can be deduced that the locus of all stable states in free energy-composition space define a continuous surface (Connolly, ms, app. B). This surface must be concave with respect to the free energy coordinate, as shown by heavy solid lines in figure 1. The equation of a line in the G-Y space represented by figure 1A can be written:

$$G = \mu_{SiO_2} Y_{SiO_2} + \mu_{CaO} Y_{CaO}, \tag{17}$$

where, from eq (14), $Y_{SiO_2} = \hat{n}_{SiO_2} (1 - Y_{CaO}/\hat{n}_{CaO})$. Thus, a line drawn through the representative coordinates of any two phases in figure 1A (such as β and η) can be extrapolated to $Y_{CaO} = 0$ and $Y_{CaO} = 1$ to obtain values of G numerically equivalent to the dependent potentials μ_{CaO} and μ_{SiO_2}. This kind of analysis is well known for G-Y space, and it can be carried out in exactly the same fashion for Ω-Y space in general. Thus, for the Ω-Y space represented by figure 1B, the equation of a line drawn through the representative coordinates of the phases β and η is:

$$\Omega = \mu_{CaO} Y_{CaO} - PY_V, \tag{18}$$

where, from eq (14), $Y_V = \hat{V}(1 - Y_{CaO}/\hat{n}_{CaO})$. If this line is extrapolated to $Y_{CaO} = 0$, the corresponding value of Ω will be numerically equivalent to the negative of the pressure consistent with the equilibrium of the phases β and η. Likewise, if the line is extrapolated to $Y_{CaO} = 1$, the value of μ_{CaO} for this assemblage is obtained.

The foregoing examples were simplified in that only phases with fixed stoichiometry and molar volume were considered. Phases with variable stoichiometry can take on an infinite number of G-Y states and, therefore, define surfaces in G-Y space. The effect of variable molar volume on phases in the Ω-Y space shown in figure 1B would be the same, that is, the possible Ω-Y coordinates of a phase with variable molar volume define a surface. In the remainder of this paper, the terms *compound* and *solution* as commonly applied in reference to chemical composition will be used in the same sense with respect to thermodynamic composition. A phase may be a compound in one composition space and a solution in another. For example, with the components $\{H, n_{SiO_2}\}$ quartz is a solution, whereas, with the components $\{V, n_{SiO_2}\}$, quartz is a compound (assuming variation in volumetric properties of quartz to be negligible).

Most readers will have an intuitive understanding of a composition such as defined by eq (15) because of the emphasis on isochemical systems in physicochemical analysis. The significance of composition as defined by eq (16) may be less clear, but such compositions are simply a

measure of the relative proportions of the conservative extensities of a thermodynamic system. The composition of a system is thus unaffected by environmental or internal processes of equilibration. In considering the isochemical system $CaO–SiO_2$, the composition expressed by eq (15) is important, because, at any fixed P-T condition, it determines the equilibrium properties $\{S, V, \mu_{CaO}, \mu_{SiO_2}\}$. In comparison, for the isochoric system closed with respect to CaO, at any given μ_{SiO_2}-T condition, the composition defined by eq (16) determines the equilibrium properties $\{S, P, \mu_{CaO}, n_{SiO_2}\}$. Because n_{SiO_2} is a dependent property in this context, it has no greater relevance in thermodynamic analysis than does a property such as the volume of an isochemical system.

Another way of understanding the significance of composition is to consider the processes of transformation from metastable to more stable phase assemblages, that is, reactions. Because composition is defined to be an invariant characteristic of a system, reactions must take place so as to conserve the amounts of each component in a system. Thus, in the isochemical $CaO–SiO_2$ system reactions conserve n_{CaO} and n_{SiO_2} but may affect the volume and entropy of the system. Whereas, in the isochoric model for this system reactions conserve n_{CaO} and V but may vary the mass of SiO_2 and the entropy of the system.

The compositions defined by eq (13) are similar to "mole fractions" which appear often in chemical literature. It is pertinent to observe, contrary to frequent assertions otherwise, that compositions cannot be unitless. This is apparent by dimensional analysis of expressions such as eq (17), for, if the compositions $\{Y_{CaO}, Y_{SiO_2}\}$ were unitless, then the potentials $\{\mu_{CaO}, \mu_{SiO_2}\}$, which have inconsistent units of energy/mole-CaO and energy/mole-SiO_2, respectively, would necessarily be additive. This would be no less absurd than asserting additivity of pressure and temperature, which may be considered (negative) mechanical and thermal potentials. Because the compositions defined by eq (13) have the same units as their extensive relatives, any thermodynamic relationship that holds for the untransformed extensive parameters, such as eq (1), can also be written in terms of compositions; however, one compositional parameter is necessarily redundant ($\Omega = f(Y_1, \ldots, Y_{c-1}, \theta_{c+1}, \ldots, \theta_n)$).

A possible point of confusion concerns the significance of the denominators in eqs (12) and (13). In both cases, the denominators are arbitrary scale factors by which the relative concentrations of extensities are measured and may be chosen entirely for convenience. Thus, in reference to a transformation of the type expressed by eq (12) Gibbs writes of the density of entropy (1957, p. 86), that is, the amount of entropy contained in a specific volume of matter. The scale in eq (13) (and for mole fractions) simply defines the extent of a system for which eq (14) is true. This scale is sometimes less useful, because it does not define a scale relative to a fundamental property. For example, given the components $\{n_{CaO}, n_{SiO_2}\}$, proportions are measured relative to an amount of matter in which n_{CaO} and n_{SiO_2} total to one, but this has no

greater physical significance than the amount of matter in which the volume and n_{SiO_2} sum to one.

The physicochemical idealization of a component is rarely realized in natural systems; moreover, the degree to which this limiting behavior is approached may vary during the evolution of a system. Consequently, the choice of whether an aspect of the state of a system should be characterized by a component or potential in a phase diagram representation is a matter of judgment and convenience. For this reason no generalized statement of the "phase rule" is made here, for such statements obscure the significance of components and perpetuate a black box treatment of phase equilibria. However, it may be noted that the equilibrium of $p > c$ phases would occur with null probability in the limit that the potentials and components of a system are specified completely independently. The recognition of this is implicit in Goldschmidt's "mineralogic phase rule" and in the writings of Korzhinskii (1959) and Zhao (1983) concerning geometrically degenerate phase fields.

CONSTRAINTS

Multivariable phase diagrams can often be simplified by the application of dimension reducing constraints. For the procedures described subsequently in this paper, any constraint must ultimately be reduced to a constraint on a potential expressed in terms of constants and/or other potentials. Such constraints can be applied in two different physicochemical circumstances. An *externally buffered* system is assumed to be in equilibrium with an infinite reservoir which contains the extensity that determines the potential of interest. The actual presence or absence of a phase containing this extensity within the system is thermodynamically irrelevant. The simplest external buffering constraint is the specification of a constant value for a potential, this is in effect sectioning a multidimensional phase diagram perpendicular to the axis representing the constrained potential. More complex constraints result in oblique and sometimes curved sections, such as when μ_{O_2} is expressed as a function of pressure and temperature, or when pressure is related to temperature by a geothermal gradient.

External buffering constraints are thermodynamically well defined. In contrast, buffering constraints are often applied to a chemical system with the assumption that the system is saturated or *internally buffered* with respect to q thermodynamic components $\{\psi_{c+1-q}, \ldots, \psi_c\}$.[5] This amounts to a vague restriction on the composition of the system which varies with the independent potentials of the system. Application of an internal buffering constraint is therefore dependent on a priori knowledge of the phase relations of a system.

[5] Internal buffering constraints can only be meaningfully applied to chemical components, for example, the "saturation" of a system with a physical component such as volume implies the phenomenological extreme $P = 0$.

The equilibrium phase on the saturation surface of a component for an internally buffered system is by definition compositionally degenerate ($Y_1 = \ldots = Y_{c-q} = 0$), as is approximately true for many oxide fluids and solids. The existence of this phase determines both the potentials $\{\theta_{c+1-q}, \ldots, \theta_c\}$ and the distribution of the components $\{\psi_{c+1-q}, \ldots, \psi_c\}$ in the equilibrium phases of a system. Consequently, in phase equilibria, it is only necessary to consider the compositional subspace $\{X_1, \ldots, X_{c-q}\}$ defined by the transformation:

$$X_j = \frac{\psi_j}{\sum_{i=1}^{c-q} (\psi_i / \hat{\psi}_i)} . \tag{19}$$

A perculiarity of internal buffering constraints is that the possible proportions of the buffered components in a system $\{\psi_{c+1-q}, \ldots, \psi_c\}$ can only be determined after a phase diagram has been calculated.

Internal buffering constraints may be applied in two different ways distinguished herein by the designations *component* and *phase saturation.* Phase saturation constraints are applied with the supposition that a specified phase is stable for all possible $\{\theta_{c+1}, \ldots, \theta_n\}$ states of interest for a system. In this case $\Omega = f(X_1, \ldots, X_{c-q-1}, Y^s_{c-q+1}, \ldots, Y^s_{c-1}, \ldots, \theta_n)$ and the compositions of the saturated phase $\{Y^s_{c+1-q}, \ldots, Y^s_{c-1}\}$ may serve as the independent variables of a phase diagram.

Component saturation constraints are applied with the supposition that at least one one-component phase, that is, a *composant* (Schreinemakers, 1965, p. 266), is stable for all possible $\{\theta_{c+1}, \ldots, \theta_n\}$ states of the system; however, the stable composant is not specified and is determined as a function of the independent potentials. Component saturation constraints are therefore specified by the identity of a component rather than a phase. Because the saturated phase contains only one component, ψ_c, the potential $\theta_c = f(\theta_{c+1}, \ldots, \theta_n)$, and $\Omega = f(X_1, \ldots, X_{c-2}, \theta_{c+1}, \ldots, \theta_n)$. The free energy function consistent with component saturation will have singularities (it is not differentiable) when two composants are in equilibrium, and these singularities are manifest as kinks in the geometric elements of phase diagrams.

Multiple component saturation constraints may be applied simultaneously; however, this can only be done if all phases within the compositional join defined by saturated components are stoichiometric compounds. In addition, if a compound is stable within this join it is evident that the simultaneous saturation of all the composants is thermodynamically inconsistent. This complication can be circumvented by the specification of a *saturation hierarchy,* which defines the relative order in which the saturation constraints are applied. As an example, consider the saturation hierarchy $\{H_2O, SiO_2, CaO\}$ and the possible phases water, quartz (SiO_2), wollastonite ($CaSiO_3$), lime (CaO), and portlandite ($Ca(OH)_2$). H_2O is the first component in the hierarchy and must therefore also be a composant. There are no compounds on the

H_2O–SiO_2 join, so quartz must also be a composant. Finally, given μ_{H_2O} and μ_{SiO_2} consistent with these composants it is then possible to determine the CaO-saturated phase, that is, lime, portlandite, or wollastonite. If the reverse hierarchy is specified, the stable saturated phases must be lime, portlandite or water, and quartz or wollastonite.

GENERALIZATION OF SCHREINEMAKERS PROJECTIONS

The projected axes in conventional Schreinemakers projections are taken to characterize the possible chemical states of a system; thus, these projections may be considered to be polychemic projections. There is no theoretical reason for this limitation of the Schreinemakers method, and it is possible to construct polythermal and polybaric projections as well (Skippen and Trommsdorff, 1975). The kind of the variable represented on a projected axes of a diagram (compositional versus potential) is not prescribed and has no effect on the geometry of a projection (Hillert, 1985a). However, projections are most useful when the projected axes can be associated with the compositional parameters of a physicochemical system. Polychemic projections are thus used for systems in which it is presumed that chemical state, or at least aspects of it, is determined by chemical composition. This presumption is consistent with the classical model of petrologic system as isochemical (Bowen, 1940); in this model environmental (petrogenetic) factors determine thermal and mechanical state, but chemical composition is an intrinsic (paragenetic) property of each system. However, it is well known that for certain magmatic and low-pressure vein-filling processes the thermal or mechanical state of a petrologic system may be determined by intrinsic properties (Korzhinskii, 1959; Thompson, 1954, 1970). More recently, it has been recognized that many petrologic systems are dynamic, and that the state of such systems may be controlled by the interaction of a system and its environment, for example "buffered" systems (Rice and Ferry, 1982), whereupon the distinction between paragenetic and petrogenetic factors is meaningless. In these instances polychemic-polythermal and polychemic-polybaric projections may prove useful. Admittedly these are special cases, and the primary motivation for introducing such projections here is to demonstrate the general character of the Schreinemakers method. Understanding this character emphasizes the thermodynamic significance of components and provides a better grounding for selecting phase diagram representations.

If the state and extent of a system are characterized by n thermodynamic properties, then the complete phase diagram of the system is $n - 1$ dimensional, because only $n - 1$ intensive properties are capable of independent variaton. For this $n - 1$ dimensional phase diagram, there are then $\binom{n}{2}$ topologically unique two-dimensional Schreinemakers projections. Three such projections are illustrated in figure 2 for CaO–SiO_2 systems. Figure 2A is the conventional polychemic projection, and B and C of figure 2 are polythermal and polybaric projections as an explicit function of μ_{SiO_2}. The projections were calculated

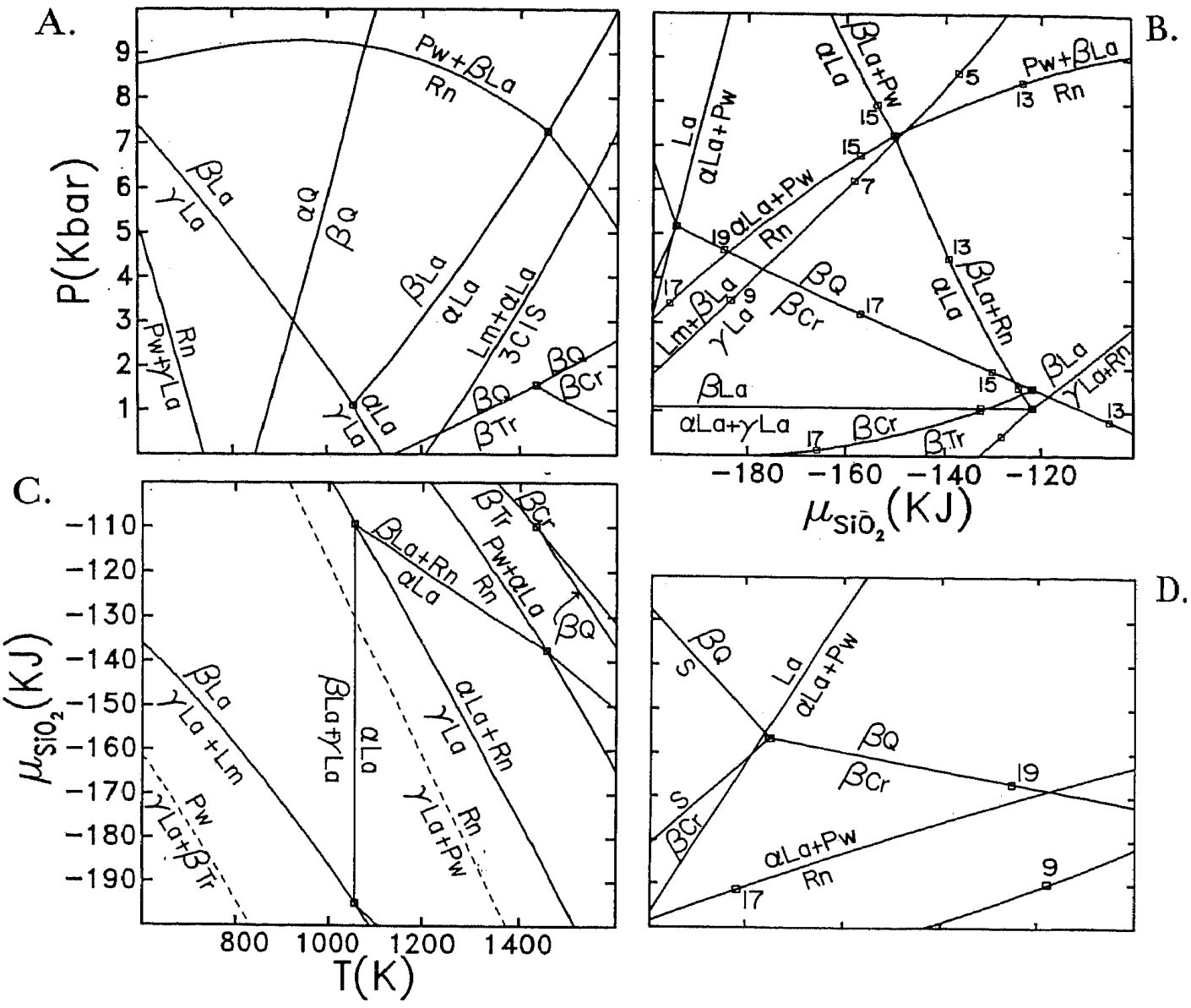

Fig. 2. Computer calculated and drafted (A) polychemic, (B) polythermal (T = 400–2200 K), and (C) polybaric (P = $-\infty$ to ∞) phase diagram projections for $CaO–SiO_2$ systems. The projections are appropriate for analysis of isochemical systems (A), adiabatic systems closed with respect to CaO (B), and isochoric systems closed with respect to CaO (C). (D) Detail of (B), for P = 3 to 7 kb and $\mu_{SiO_2} = -200$ to -180 kJ/mol. In (B) curves are labeled at intervals by equilibrium temperature in hundreds of Kelvins. Dashed curves in (C) are imaginary phase fields in equilibrium at negative pressures. Greek letters are used as prefixes on phase names to indicate different polymorphs. Data from Berman and Brown (1984).

(using methods discussed later) by computer with the data of Berman and Brown (1984) assuming invariant volume and stoichiometry for the equilibrium phases. Note that some of the phase fields in figure 2 may be metastable with respect to phases, such as $CaO–SiO_2$ melt and vapor, for which thermodynamic data are lacking.

If the projected axis of the three-dimensional $CaO–SiO_2$ phase diagram is taken to represent a compositional parameter, a different composition space can be associated with each projection in figure 2. For the projections shown in figure 2A through C the components may be

taken, respectively, as $\{n_{CaO}, n_{SiO_2}\}$, $\{n_{CaO}, S\}$, and $(n_{CaO}, V\}$. Because of the assumptions of invariant volume and stoichiometry, the phases represented in figure 2A and C may be considered compounds. The composition of a compound is implicit in its definition, thus the dependent potentials (that is, μ_{CaO}, and μ_{SiO_2} or P) in any phase field of figure 2A and C are completely determined by the projection coordinates. In contrast, the thermal state of any phase can be varied independently of its mass, so in the composition space defined by the components $\{n_{CaO}, S\}$ all phases that contain CaO must be treated as solutions. Consequently, some information, in addition to the identities of the equilibrium phases, must be provided to characterize completely the state of the system in a phase field. In figure 2B this information is provided by indicating the temperature at intervals on the univariant curves. It should be noted that if the entropy is regarded as a component, the thermal state of the system is considered to be determined by its entropy, and temperature is a dependent property. Despite this, temperature was used to characterize thermal states in figure 2C because it is the more familiar thermal variable.

For figure 2A the independent compositional variable, X_{CaO} may be defined as in eq (15), and the projection is of all compositions such that $\{0 \leq X_{CaO} \leq 1\}$. It happens that over the entire range of coordinates represented in the projection, the equilibrium states correspond to possible physical states but it is not uncommon that components may be selected for which this is not true and that the composition represented by a pure component corresponds to an imaginary state. This is the case for the components specified for figure 2C, from which the independent compositional variable, X_{CaO}, is defined as in eq (16). As with figure 2A, figure 2C is a projection of the compositions $\{0 \leq X_{CaO} \leq 1\}$, however, for compositions defined by eq (16) the compositional extremes correspond to the physical extremes of infinite volume and mass.[6] Therefore, although all the phase fields of figure 2C satisfy condition (2) it can be deduced, by comparison with figure 2A, that the fields {Pw, γLa, βTr} and {Rn, γLa, Pw} must occur at imaginary pressures ($P < 0$). Even though these fields are not possible in real systems, they are shown because they restrict the possible equilibrium μ_{SiO_2}-T states of assemblages containing rankinite or pseudowollastonite.

The calculation of the projections in figure 2A and C is relatively simple because the free energy of a compound can be expressed entirely in terms of the independent potentials of a system, that is, for figure 2A and 2C $\Omega^i = f(T, P \text{ or } \mu_{SiO_2})$. In contrast, each CaO-bearing phase in figure 2B is a binary solution for which $\Omega^i = f(X^i_{CaO}, P, \mu_{SiO_2})$, where:

$$X_{CaO} = \frac{n_{CaO}}{n_{CAO}/\hat{n}_{CaO} + S/\hat{S}}. \tag{20}$$

[6] If n_{CaO} is regorously zero, that is in a pure SiO_2 system, the molar volume of the system is not independently variable, and the system has no compositional degrees of freedom; thus pure SiO_2 systems are excluded from consideration here.

Thus, in the calculation of projections it is necessary to specify a compositional range for each solution. Conventionally for chemical solutions this is done by specifying endmember compositions from phenomenological considerations; however, there is no phenomenological basis for defining "end-member" thermal states. For the calculation of figure 2B it was therefore necessary to specify an arbitrary set of endmember states for each solution; these states were taken to be characterized by temperatures of 400 and 2200 K. As a result of this arbitrary definition, figure 2B represents only thermal states within this range of temperatures.

An interesting feature of the different projections in figure 2 is that a phase field that is geometrically degenerate in one projection may be nondegenerate in another. For example, the field {αLa, βLa, γLa} is invariant in figure 2A, but is univariant in both figures 2B and C, and would be divariant in a polythermal-polybaric projection. This occurs because chemically degenerate phases are compositionally nondegenerate in the composition space appropriate for the analysis of a polythermal or polybaric projection.

PART II. AUTOMATED CONSTRUCTION OF MULTIVARIABLE PHASE DIAGRAMS

Calculation of a phase diagram and calculation of an individual equilibrium state are problems of a different scale, for a phase diagram represents the infinite number of possible stable states of a system characterized by the variable parameters $\{X_1, \ldots, X_{c-1}, \theta_{c+1}, \ldots, \theta_n\}$.[7] The phase diagram problem is thus a problem of strategy in that it is necessary to devise an efficient scheme to outline the stable phase fields of a diagram. Many procedures have been developed for automating, in part or entirely, phase equilibrium and phase diagram calculations; to place the work presented here in perspective it may be useful to review these procedures.

REVIEW OF COMPUTATIONAL METHODS

The characterization of the equilibrium phases of a system specified by invariant state coordinates, that is, calculation of an individual equilibrium state, is a problem that has been addressed extensively (Zeleznik and Gordon, 1968; Van Zeggeren and Storey, 1970; Eriksson, 1971; Brown and Skinner, 1974); more recent contributions have achieved a high level of sophistication with regard to the thermodynamic models that may be employed (Hillert, 1981b; Lukas, Weiss, and Henig, 1982; Eriksson and Hack, 1984). These techniques can be used to calculate phase diagrams by incrementally varying the state coordi-

[7] The compositional variables of a saturated phase are directly related to potentials; consequently, calculations and diagram topologies as a function of the composition of a saturated phase are essentially identical to potential variable calculations and diagram topologies. Therefore, for brevity, the compositional variables of saturated phases are not distinguished here from potentials.

nates of a system and determining the equilibrium phase assemblage at each new set of coordinates. The resulting assemblages are assigned to the different phase fields, and the field boundaries can be determined by iteration or interpolation. The advantage of such a procedure is that it is easy to implement, and that there are no constraints on the nature of the coordinate pattern used. These methods have been applied in the calculation of composition sections of multicomponent petrologic systems (Brown and Skinner, 1974; Saxena and Eriksson, 1983; Wood and Holloway, 1984; DeCapitani and Brown, 1987).

An alternative to incremental mapping is to define phase field boundaries directly. This can be done in two ways: (1) all possible boundaries are calculated, and then the most stable boundaries are selected; or (2) the equilibrium phases are determined as the saturation surface of a specified phase is traced. Method (1) is used by Kaufman and Bernstein (1970) for alloy systems and is flexible, but not easily completely automated. Method (2) is usually implemented with the assumption that the saturated phase is stable, as in the calculation of liquidus surfaces (Lin and others, 1980; Berman and Brown, 1984). Jansson (cited in Hillert 1981b) has developed a particularly effective technique after method (2) in which free energy minimization techniques are coupled with the auxiliary constraint that the extent of a specified stable phase is zero. With Jansson's modification boundaries can also be traced in composition sections. By testing the stability of the equilibrium phases as boundaries are traced, the stable phase fields of a diagram can be defined. Such a strategy is used for the completely automated phase diagram calculations described by Sundman, Jansson, and Anderson (1985).

In comparison to the incremental mapping of phase fields, the tracing of phase field boundaries is considerably more efficient. However, for coordinate grids of greater than two dimensions the efficiency of both methods decreases drastically and the likelihood that a phase field will be missed entirely increases; therefore, some expertise is needed to assure that a correct diagram is calculated. Because of these complications, it is necessary to employ alternative strategies for multivariable phase diagrams. Multivariable phase diagrams are usually shown as Schreinemakers projections; consequently, previous computational strategies have been designed for the direct calculation of projections rather than complete multidimensional phase diagrams.

The strategy used by Hillert (1981b; see also Lukas and others, 1982; Hillert, 1982) for calculating Schreinemakers projections is to determine initially a stable invariant equilibrium condition at which n ($n = c + 2$) phases are stable. This condition serves as a starting point from which at least three and at most n stable univariant phase fields can be traced. Each univariant field may terminate at a new invariant condition which, in turn, can be used to generate additional univariant fields. This strategy has been completely automated in a computer program which can treat solution phases described by Margules expan-

sions and any number of components (Hillert, personal commun., 1986). It is not certain that the loci of univariant conditions will form a continuous network within the parametric space of the diagram. It is therefore necessary to test the stability of all possible invariant configurations to assure that stable configurations are not overlooked. Such testing may result in a significant deterioration in efficiency if the number of potentially stable phase (π) is much greater than n, because the number of invariant phase configurations is the combinatorial function $\binom{\pi}{n}$. This situation is further complicated by the possibility that the same invariant phase assemblage may be stable at more than one condition, as sometimes observed (Skippen, 1971; Trommsdorff, 1972; Day, Chernosky, and Kumin, 1985). A second difficulty is that univariant curves that do not begin or end at an invariant point within the specified coordinate frame will not be determined.

Perkins, Brown, and Berman (1986) used a similar technique for stoichiometric phases that eliminates the possibility for errors of omission and was specifically designed for geologic problems. Instead of enumerating invariant phase assemblage the strategy of Perkins, Brown, and Berman begins with univariant assemblages. This has the disadvantage that it is necessary to test the stability of each assemblage over the entire range of its equilibrium coordinates within a diagram, rather than at a single condition as required in Hillert's strategy. Additionally, the number of univariant assemblages generated by combinatorial enumeration, $\binom{\pi}{n-1}$, is generally greater than the number of invariant assemblages (if $\pi > 2n + 2$). Thus, although this strategy is completely reliable, it is less efficient than Hillert's, and its use is restricted to systems in which the possible phases have no compositional degrees of freedom.

COMPUTATIONAL STRATEGY OF THE VERTEX PROGRAM

The program presented here, called Vertex, was initially developed with the specific goal of automating the calculation of Schreinemakers projections. Inasmuch as the difficulties inherent in a purely combinatorial approach to the calculation of projected diagrams are well known, attention was directed toward the calculation of complete multidimensional phase diagrams. In calculating a phase diagram, as opposed to a phase diagram projection, it is simple to determine when the diagram is complete, because the volume of the different phase fields must fill the entire parametric space prescribed for the diagram. Thus the necessity of testing the stability of all possible phase fields can be avoided. Additionally, because neighboring phase fields differ by only one phase (Palatnik and Landau, 1964; Zhao, 1983), by systematically building up a diagram, the number of permutations of phases considered to define a field is diminished. This is particularly important in completely automated calculations, because the number of potentially stable phases is generally large.

The strategy used in Vertex is almost the antithesis of Hillert's (1981b) strategy for calculating Schreinemakers projections. Hillert's strategy begins with invariant phase fields, whereas the Vertex strategy begins by establishing isopotential one-phase one-component phase fields. The compositional degrees of freedom are then successively incremented. After each increment the compositional phase relations of increasing complexity are established, until ultimately a complete composition diagram is determined. A degree of freedom is then introduced in one potential variable, and the compositional phase relations are then monitored as this potential is varied. The invariant phase fields determined in this manner can then be traced as a function of a second potential to trace the networks of univariant phase fields which comprise a Schreinemakers projection.

The calculation of multidimensional phase diagrams by the strategy outlined for Vertex is divided into three steps, and the result of each step can be a complete diagram. The first step produces an isopotential composition phase diagram, and the second and third steps produce mixed-variable diagrams as a function of composition and one and two potentials, respectively. Diagrams with two potentials are almost invariably shown in projection and will be referred to as Schreinemakers diagrams. The following three sections outline the methods used for each kind of diagram, thereby detailing the overall strategy.

COMPOSITION PHASE DIAGRAMS

The problem in calculating composition phase diagrams is to determine the phase assemblages that define the thermodynamic surface of a system, that is, the isopotential locus of possible minimum free energy-composition (Ω-X) states. In the most general case, in which all phases are of variable composition, this task is not straightforward because the free energy of a system depends both on the composition of the system and its phases. A more important, though less apparent, difficulty is that the geometry of the Ω-X surface may be complex and difficult to describe analytically. Such a description is essential if the phase relations on this surface are to be monitored as potentials are varied.

The complications mentioned in the previous paragraph combine to make numerically exact evaluation of the thermodynamic surface of complex systems untenable by current techniques. However, in some cases the compositional variation of phases is negligible, and the evaluation of thermodynamic surfaces is greatly simplified. This simplified problem is relevant to some subsolidus silicate systems and was addressed initially in the development of Vertex. If the only possible phases of a system are compounds, the thermodynamic surface of the system is a hull-shaped simplicial complex concave with respect to the free energy ordinate. The vertices of this complex correspond to the coordinates of the stable compounds, and each simplicial facet of the complex is an invariant phase region.

The coordinates of any p = c compositionally nondegenerate phases define a plane in Ω-X space which is described by the equation:

$$\Omega = \sum_{j=1}^{c} \theta_j X_j. \tag{21}$$

The potentials in eq (21) must satisfy:

$$\begin{pmatrix} X_1^1 & \cdot & \cdot & X_c^1 \\ \cdot & \cdot & \cdot & \cdot \\ \cdot & \cdot & \cdot & \cdot \\ X_1^p & \cdot & \cdot & X_c^p \end{pmatrix} \begin{pmatrix} \theta_1 \\ \cdot \\ \cdot \\ \theta_c \end{pmatrix} = \begin{pmatrix} \Omega^1 \\ \cdot \\ \cdot \\ \Omega^p \end{pmatrix} \tag{22A}$$

or

$$\bar{X}\,\bar{\theta} = \bar{\Omega} \tag{22B}$$

which can be solved for $\bar{\Omega}$ by standard linear algebraic techniques. If an invariant assemblage is stable, then the Ω-X plane defined by eqs (21) and (22) must be tangent to the thermodynamic surface of the system; thus, the residual free energy $\delta\Omega^i$ of all phases relative to this plane must be positive, that is:

$$0 \leq \delta\Omega^i = \Omega^i - \sum_{j=1}^{c} \theta_j X_j^i \qquad (i = 1, \ldots, \pi). \tag{23}$$

Eqs (22) and (23) provide the basis for a simple algorithm for the evaluation of the thermodynamic surface of a system. This algorithm consists of essentially three steps: (1) invariant assemblages are generated, (2) for each assemblage eq (22) is solved for $\bar{\theta}$, and (3) the validity of condition (23) is tested. If the only phases of a system are compounds a set of algebraic rules can be formulated to limit the number of assemblages that must be tested in this manner to a small fraction of the total possible number $\binom{\pi}{c}$. As a result the algorithm, which has been described in detail elsewhere (Connolly and Kerrick 1987), is surprisingly efficient.

Because of the efficiency of the algorithm, it is feasible to model the nonlinear Ω-X surfaces of phases with variable composition by a series of compound phases. This is equivalent to approximating each surface by an inscribed polyhedron, the vertices of which correspond to arbitrarily defined compounds. Any desired degree of accuracy in this approximation can be achieved by varying the number of compounds, although in practice the accuracy for solutions with more than three endmembers is limited by the amount of computer memory required. All phase regions on the thermodynamic surface are defined by c compounds as a result of this approximation; however, once these regions have been defined it is possible to determine the true phase relations by determining if more than one of the compounds represents a single solution. Because it is also

possible to recognize immiscibility in a solution, this technique provides an effective means of defining solvi in complex systems (Connolly and Kerrick, 1987). To emphasize that the compounds chosen to represent a particular solution are arbitrarily defined, they will be referred to as *pseudocompounds.* Similarly, to distinguish the true variance of a phase region from the variance of a region defined by pseudocompounds, the term *pseudovariance* will be applied in the latter case. The subdivision of phases into pseudocompounds, and the interpretation of the phase relations calculated as a result, can be accomplished entirely by computer programs and need not concern users.

Figure 3 shows a composition phase diagram calculated by computer for the chemically closed system $CaO–Al_2O_3–SiO_2$ at a temperature roughly 200 K above the solidus. Three different kinds of phase regions can be distinguished in the diagram: divariant melt regions are shown by shading, univariant regions are defined by dashed tielines, and invariant phase regions are outlined by solid lines. Within the melt regions, the pseudoinvariant phase regions are also outlined. The

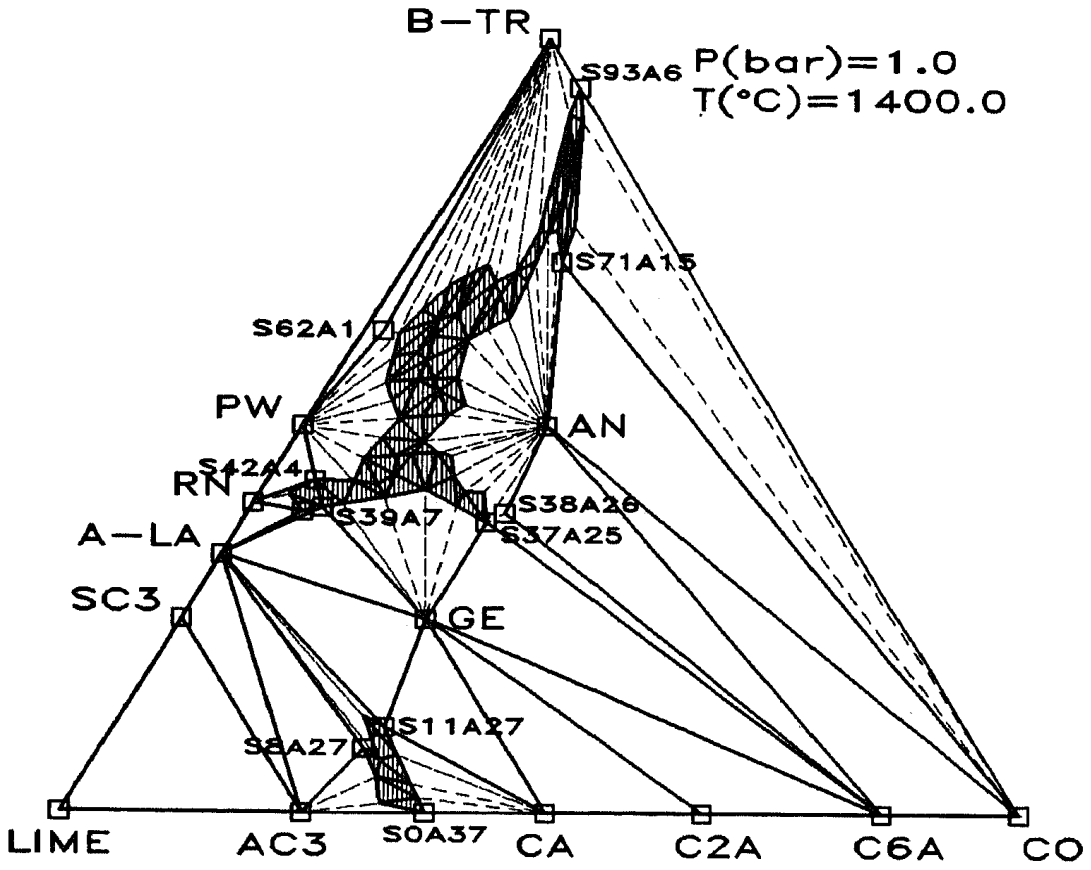

Fig. 3. Computer calculated and drafted composition phase diagram for $CaO–SiO_2–Al_2O_3$ supersolidus systems (P = 1 bar, T = 1673 K). Three kinds of phase regions are distinguished: divariant melt regions by shading, univariant melt-solid regions by dashed tielines, and invariant three phase regions outlined by solid lines. Within melt regions, pseudoinvariant regions are also outlined. Numbers in symbols should read as subscripts (for example, S71A15 is $S_{71}A_{15}$). Polymorph types are indicated by an arabic letter prefix. Data from Berman and Brown (1984).

calculation, in which the melt phase was represented by 700 compounds, involved a total of 733 compounds and consumed 0.17 seconds of CPU time.[8] Had this calculation been done by brute force enumeration of pseudocompound assemblages, the calculation would have involved nearly one million assemblages.

Mixed-variable Phase Diagrams

Mixed-variable phase diagrams show changes in compositional phase relations as a function of one independent potential. Ordinarily the calculation of mixed-variable phase diagrams is not a simple task, because the geometry of high variance phase regions ($p \leq c$) usually varies continuously in such diagrams. However, if the only phases of a system are compounds, all geometric variations are discrete and manifest in the topology of mixed-variable diagrams. Topologic changes are associated with invariant equilibria and can be defined by a reaction equation that relates the compositions of the coexistent phases. The approximation of solutions by pseudocompounds results in such a situation but, in this case, it is possible to distinguish reactions that involve compounds representing different phases from those in which two or more pseudocompounds represent a single homogeneous phase. Reactions of the former kind correspond with topologic changes and heterogeneous invariant equilibria in a true phase diagram, whereas, reactions of the latter kind approximate the continuous variation of a homogeneous phase region. Given isopotential phase relations for a system, the location of the conditions at which reactions occur as a function of one potential is then sufficient to determine the geometry of a mixed-variable diagram.

The most obvious strategy for locating the conditions at which reactions occur is to vary one potential and then to test the stability of the original univariant (or pseudounivariant) phase assemblages. This strategy was implemented in preliminary versions of Vertex (Connolly and Kerrick, 1984, 1987), and although intuitively appealing, it has practical shortcomings. These shortcomings arise because one reaction may affect the stability of many univariant assemblages, and this situation must be distinguished from one in which more than one reaction occurs within a finite potential increment. The formulation of criteria for distinguishing these situations is a formidable problem in combinatorial topology (Hudson, 1959). This problem was solved for one-, two-, and three-component systems, but the resulting criteria could not be generalized for higher order systems.

An alternative strategy is to evaluate the stability of each univariant assemblage individually as a function of the potential variable θ_v.

[8] Calculations reported here were done on an IBM 3090-180 computer (clock speed 18.5 Ns) running under VM/SP (HPO level 4.2). The capabilities of this computer are typical of main frame computers currently available at most universities; however, CPU time consumption may vary by orders of magnitude, depending on the operating system, clock speed, and compilers used.

Reactions are identified when an originally stable assemblage is metastable with respect to one phase, designating this phase by the index p (p = c + 1), the reaction equation may be written:

$$\vec{\phi}_p = \sum_{i=1}^{c} \alpha_i \vec{\phi}_i, \tag{24}$$

where $\vec{\phi}_i$ is the composition vector of the i^{th} phase and is usually designated by the name of the phase. The reaction coefficients $\{\alpha_1, \ldots, \alpha_c\}$ may be determined from:

$$\begin{pmatrix} X_1^1 & \cdot & \cdot & X_c^1 \\ \cdot & \cdot & \cdot & \cdot \\ \cdot & \cdot & \cdot & \cdot \\ X_c^1 & \cdot & \cdot & X_c^c \end{pmatrix} \begin{pmatrix} \alpha_1 \\ \cdot \\ \cdot \\ \alpha_c \end{pmatrix} = \begin{pmatrix} X_1^p \\ \cdot \\ \cdot \\ X_c^p \end{pmatrix} \tag{25A}$$

or

$$\bar{X}^t \vec{\alpha} = \vec{\phi}_p, \tag{25B}$$

where $\bar{X}^t$ is the transpose of the composition matrix of eq (22). The value of the independent potential variable θ_v for the invariant equilibrium associated with the reaction must satisfy:

$$\sum_{i=1}^{p} \alpha_i \Omega^i(\theta_v) = \Delta\Omega(\theta_v) = 0, \tag{26}$$

where the functional dependence of Ω is indicated parenthetically, and, from eq (24), it follows that $\alpha_p = -1$.

Eq (26) can be solved to any desired accuracy by numerical techniques. For this purpose, the secant method (Conte and DeBoor, 1980) is superior to other methods, because it does not require that Ω be analytically differentiable. The input for the secant method is an initial estimate for the value of the independent potential θ_v^o and an arbitrary increment $\delta\theta_v$. The equation:

$$\theta_v = \theta_v^0 - \frac{(\Delta\Omega(\theta_v^o))\delta\theta_v}{\Delta\Omega(\theta_v^o + \delta\theta_v) - \Delta\Omega(\theta_v^o)} \tag{27}$$

is then solved for θ_v. If θ_v is sufficiently close to θ_v^o or $\Delta\Omega(\theta_v^o)$ is close to zero, θ_v is accepted as a solution to eq (26). Otherwise θ_v is made the new estimate, θ_v^o, and the procedure is repeated until the convergence criteria are met.

Once an invariant phase boundary has been located by solving eq (26), the stable univariant phase regions on the opposite side of the boundary from the region defined by the original assemblage $\{\vec{\phi}_1, \ldots, \vec{\phi}_c\}$ must also be determined. The regions can be defined by the method just described, but first it is necessary to determine the stable assemblage

in each region, that is, assemblages that may be generated by the reaction of the original assemblage $\{\vec{\phi}_1, \ldots, \vec{\phi}_c\}$ with the phase $\vec{\phi}_p$. These assemblages can be enumerated by noting that phases with null reaction coefficients must be compatible with all phases of the invariant assemblage on either side of the invariant boundary, and phases with negative reaction coefficients must be compatible with each other on the opposite side of the boundary from $\{\vec{\phi}_1, \ldots, \vec{\phi}_c\}$. Thus, phases with null and negative coefficients will be present in all possible assemblages generated by the reaction from $\{\vec{\phi}_1, \ldots, \vec{\phi}_c\}$. Of the remaining k phases with positive reaction coefficients only k-1 at a time may coexist. Provided k is greater than one, the invariant reaction will therefore generate k new stable univariant assemblages, each of which consists of a permutation of k-1 phases with positive coefficients plus all phases with null or negative coefficients. If only one phase has a positive coefficient, this phase is unstable on the opposite side of the invariant boundary from $\{\vec{\phi}_1, \ldots, \vec{\phi}_c\}$.[9]

The procedure for locating invariant conditions must be repeated for every univariant or pseudounivariant assemblage defined in the initial composition diagram. Because a reaction may generate the same univariant assemblage from up to c distinct original assemblages, a large number of redundant calculations may be done. This problem can be avoided by applying tests for redundancy in programs based on the algorithm.

The result of this procedure consists of a list of invariant (and pseudoinvariant) conditions and the assemblages. To construct a phase diagram from these data, the invariant conditions must first be sorted with respect to θ_v. Because the univariant phase regions are known from the initial composition diagram calculation, these regions can be drawn parallel to the θ_v axis of the diagram to the first invariant boundary. At this condition it is necessary to determine the topology of the new univariant regions relative to the invariant boundary. The new regions can then be drawn to the next invariant condition. This process is repeated until the diagram is complete. In this construction, which may be accomplished by computer, the curvature of phase region boundaries is represented by a series of steps, where each step is defined by a pseudoinvariant condition (figs. 10 and 12, Connolly and Kerrick, 1987). These stepped boundaries may be fit with spline functions to obtain smoothed curve approximations for graphical representation.

Figure 4 shows a mixed-variable phase diagram calculated with Vertex for the CaO–SiO_2 system. The diagram can be thought of as an isopotential section of the phase diagram represented by projection in

[9] This procedure has a basis similar to Fujii's (1977) Divariant Region Theorem. Inasmuch as there are only a finite number of possible chemographic arrangements of c+1 phases, it seems that it should be possible to employ this method to determine the unique chemographic relations of c+2 phases and, therefore, the number and topology of possible invariant configurations in Schreinemakers projections.

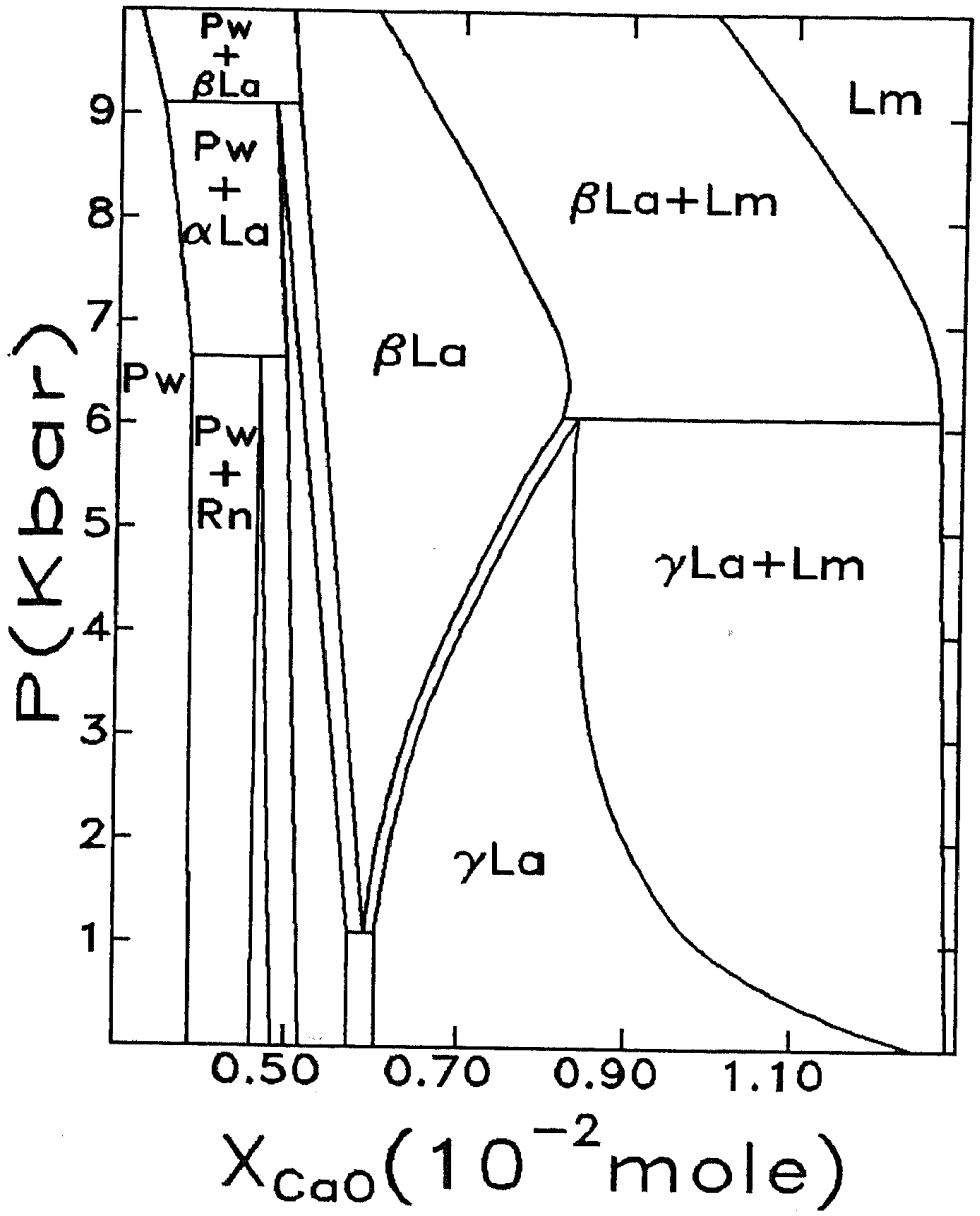

Fig. 4. Computer calculated and drafted P-X_{CaO} diagram for CaO-SiO_2 system, at constant $\mu_{SiO_2} = -160$ kJ/mol. X_{CaO} is defined by eq (20) and is similar to the inverse of molar entropy. Lines of constant X_{CaO} are isentropic. Data from Berman and Brown (1984).

figure 2B for which composition (X_{CaO}) is defined as in eq (20). This diagram is appropriate for the analysis of a physicochemical system in which the mass of lime and the thermal state are or are determined by properties of the system, but silica chemical potential and pressure are externally controlled. The variable X_{CaO} is closely related to the reciprocal of the molar entropy, and figure 4 can be interpreted accordingly, that is, low and high values of X_{CaO} are, respectively, cold and hot conditions, and the extremes $X_{CaO} = 0$ and $X_{CaO} = 1$ correspond, respectively, to the phenomenological extremes of {$T = \infty$ K, $\mu_{CaO} = -\infty$ J/mol} and {$T = 0$ K, $\mu_{CaO} = 0$ J/mol}. Calculations by Vertex are necessarily done over the entire compositional range represented by the

selected components; however, valid thermodynamic data may be available over only a portion of this range, and only this portion of a diagram will represent real phase relations. The phase relations shown by figure 4 represent thermal states characterized by temperatures within the range 400 to 2200 K.

Lines of constant composition (*isopleths*) in figure 4 are equivalent to isentropics and, by eqs (9) and (11), adiabats. The use of the term adiabat in this context is equivocal because figure 4 represents states of constant μ_{SiO_2} (−160 kJ/mol), which could be maintained only in a system open with respect to silica. However, the concept of heat in chemically open systems is vaguely defined; the equation of isopleths and adiabats in figure 4 is consistent with the concept of heat often used in physics (Born, 1964, p. 146; Tisza, 1966, p. 113) but is inconsistent with the definitions implicit in the usage of Gillespie and Coe (1933) and Tunell (1977), which may be more relevant to natural systems. This situation is further complicated because it is difficult to imagine a process by which μ_{SiO_2} could be controlled independently of the thermal state and pressure of a system. Despite the questionable relevance of figure 4 to a natural system, the diagram was presented because it is interesting from a theoretical perspective and because it demonstrates the feasibility of problems involving a large number of solution phases. It is pertinent to observe that adiabatic mass transfer is realized by superfluids (London, 1954, p. 72), and in some natural magmatic systems the transfer of low-molecular weight volatiles may occur with negligible thermal effect.

Figure 4 was calculated taking into account 37 possible phases. Each phase was represented as a binary solution as a function of X_{CaO} by 20 pseudocompounds in the compositional range shown in the diagram. The calculation of the diagram involved the evaluation of over 100 invariant conditions and consumed a total of 1.2 sec of CPU time.

Schreinemakers Diagrams

Each invariant phase boundary in a mixed-variable phase diagram corresponds to a point on a univariant field of a Schreinemakers projection. Thus, if mixed-variable diagrams are calculated which correspond to each boundary of the rectangular θ_{c+1}-θ_{c+2} coordinate frame of a Schreinemakers diagram, then the intersections of all the univariant curves in the Schreinemakers diagram with the boundary of the diagram are known. Each of these intersections may then serve as a starting point from which it is possible to trace a Schreinemakers net. Many of the invariant conditions detected in the mixed-variable diagrams will often be related by a single net, so typically, it is necessary to determine only a few nets to establish a complete Schreinemakers diagram.[10]

[10] This strategy is based on the assumption that every Schreinemakers net intersects the coordinate frame boundary at least once. Exceptions to this are rare but could occur in a system in which both ends of a unvariant field are critical points.

A curve in a Schreinemakers diagram represents the locus of a univariant equilibrium of c + 1 phases as a function of two potentials, θ_{c+1} and θ_{c+2}. This equilibrium can be associated with a reaction equation (eq 24) which is found from eq (25). Consequently, it is possible to trace the conditions of the equilibrium by incrementing one potential and then iteratively solving, by the secant method (eq 27), for the value of the other potential which satisfies eq (26). There are two special cases that may be encountered in tracing a univariant curve. First, the slope of a univariant curve may equal or approach zero with respect to the independent potential coordinate in which case $(\partial\Delta\Omega/\partial\theta_v)_{\psi_{i,1\le i\le c}\theta_{i,i\ne v,c<i\le n}}$ will also approach zero and the secant method will fail to converge. If this occurs, the independent and dependent potentials must be interchanged, and the direction of the tracing as a function of the new independent potential is determined from the generalized Clausius-Clapeyron relation:

$$\left(\frac{\partial\theta_{c+1}}{\partial\theta_{c+2}}\right)_{\psi_{i,1\le i\le c},\theta_{i,c+2<i\le n}} = \left(\frac{\partial\Delta\psi_{c+2}}{\partial\Delta\psi_{c+1}}\right)_{\psi_{i,1\le i\le c},\theta_{i,c+2<i\le n}} \tag{28}$$

The second special case occurs if a univariant curve ends at a critical point; such conditions are easily identified because the ratio in eq (28) is undefined at the critical point.

Each univariant equilibrium defines a condition at which the representative coordinates of the c + 1 phases are coincident with a plane in Ω-X space. The equation of this plane (eq 21) may be determined from eq (22) from any compositionally nondegenerate subset of c of the c + 1 phases in the equilibrium assemblage.[11] If the equilibrium is stable, condition (23) must be true given the potentials consistent with eqs (21) and (22).

A univariant assemblage may be stable over the entire range of its equilibrium conditions within the coordinate frame of a Schreinemakers diagram. Alternatively, in the course of tracing the corresponding univariant curve, an invariant point may be crossed in which case condition (23) will be false. The invariant point may then be found by locating conditions along the univariant curve at which the equality in condition (23) is true for one other phase in addition to the c + 1 phases of the univariant assemblage. If the c + 2 phases stable at the conditions represented by the invariant point are compositionally nondegenerate there will be c + 2 univariant curves emanating from the invariant point, one of which is already traced. Each of these curves will represent the equilibrium of c + 1 phases and may be defined by taking the unique c + 1 phase permutations of the invariant assemblage. The reaction equation for each univariant assemblage may then be determined, and

[11] Once $\bar{\bar{X}}$ has been factored the first time, the upper and lower triangular decompositions of $\bar{\bar{X}}$ may be stored so that subsequent solutions of eq (22) can be obtained by back substitution (Conte and DeBoor, 1980). Consequently, there is relatively little computational overhead associated with testing the stability of a univariant equilibrium.

the univariant curves traced. If these curves in turn terminate at invariant points, the invariant assemblages and conditions may be recorded, and subsequently the curves emanating from these points may also be traced. Ultimately this procedure will determine a complete Schreinemakers net within the specified potential variable coordinate frame.

If an invariant phase assemblage is compositionally degenerate the possibility exists that (1) there may be less than c + 2 univariant equilibria associated with the invariant condition, and/or (2) the same reaction equation may be associated with two or more of the univariant equilibria. Condition (1) is a manifestation of complete degeneracy between two or more phases in the invariant assemblage, and, consequently, at least one c + 1 phase permutation of the invariant assemblage will not define a c-dimensional region of composition space. This condition is detected if the row rank of the skew matrix formed by the c + 1 column vectors $\{\vec{\phi}_1, \ldots, \vec{\phi}_{c+1}\}$ is less than c, and the assemblage is rejected as a possible equilibrium. Condition (2) is the result of a linear degeneracy among three or more phases; in this case all c + 1 phase permutations (which do not involve completely degenerate phases) are possible equilibria. In these cases each univariant curve must be traced independently, even though curves associated with the same reaction equation may overlap, because in general, the curves will terminate at different invariant points.

Much of the efficiency of Vertex derives from the approximation of solution phases by pseudocompounds. As a result of this approximation, the reaction coefficients associated with a univariant equilibrium $\{\alpha_1, \ldots, \alpha_{c+1}\}$ only change when there is a change in the pseudocompound assemblage that represents the true phase assemblage. These changes appear as singularities, or pseudoinvariant points, along a univariant curve, and they represent conditions at which two pseudocompounds of the same true phase are stable. This is demonstrated in figure 5 which shows the topology of a Schreinemakers diagram for a binary system with four possible phases, three of which {A, B, D} are stoichiometric, and the fourth phase, C, is a solution represented by three pseudocompounds $\{C_1, C_2, C_3\}$. The univariant curve that corresponds to the true assemblage {A, B, C} is defined by the assemblage $\{A, B, C_2\}$ in the vicinity of the invariant point I. As this curve is traced away from the invariant point I eventually the pseudoinvariant point II is encountered.[12] This point represents conditions where the continuous compositional variation of phase C is approximated by a discrete change between the pseudocompounds C_2 and C_3. The assemblage $\{A, B, C_3\}$ then defines the univariant curve as it is traced on the other side of point II.

[12] The terms pseudounivariant curve and pseudoinvariant point are strictly incorrect, because points and curves are by definition univariant and invariant, respectively. These terms are used here for brevity in place of the more proper terms pseudounivariant equilibrium curve and pseudoinvariant equilibrium point.

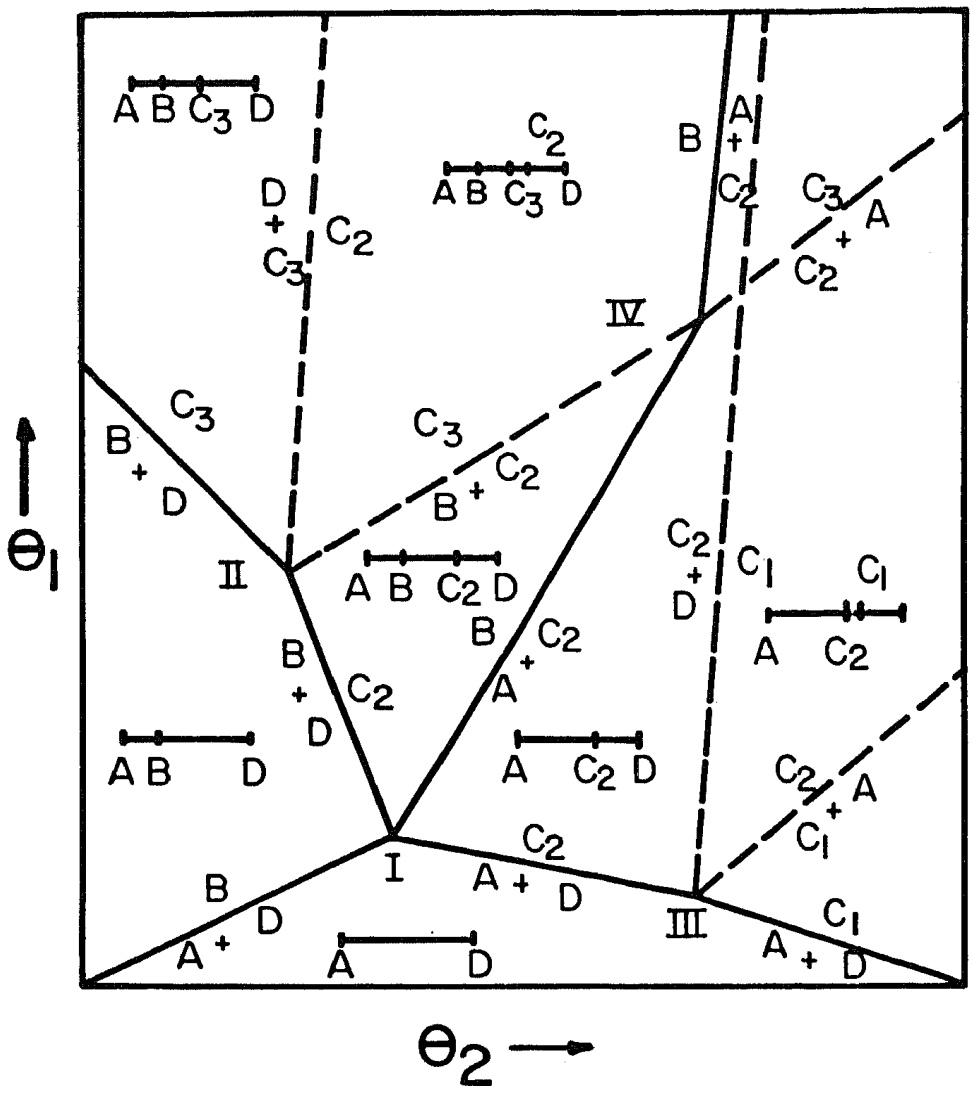

Fig. 5. Schematic Schreinemakers diagram for a two-component system with four stable phases {A, B, C. D}, where C is a solution represented by three pseudocompounds {C_1, C_2, C_3}. Univariant and pseudonivariant curves are shown by solid and dashed curves, respectively. Composition diagrams illustrate phase compatibilities in different portions of the Schreinemakers net.

In addition to the univariant pseudocompound assemblages associated with a pseudoinvariant point on a univariant curve, there are also c pseudounivariant assemblages. Each of these assemblages includes two compounds that represent the same real phase and may be used to define a pseudounivariant curve in a Schreinemakers diagram. These curves approximate the loci of conditions in which the limiting compositions of the phases of a high variance ($c-p \geq 0$) equilibrium are the same. Thus, pseudounivariant curves approximate isoplethal contours of high variance phase region boundaries. For example, the pseudounivariant curves associated with pseudounivariant point II in figure 5 correspond to the equilibrium of the pseudocompound assemblages {B, C_2, C_3} and {D, C_2, C_3}. These curves define the limiting composition of phase C in divariant equilibrium with phases B and D, respectively, as a

function of θ_{c+1} and θ_{c+2}. In this example, the one-phase region of C is only trivariant and is therefore also defined by the pseudounivariant curves.

In more complex problems than those illustrated by figure 5, pseudounivariant curves may intersect at pseudoinvariant points that do not lie on univariant curves. The pseudounivariant curves at these intersections generally define higher variance phase regions, such as divariant phase regions (binary solvi) which separate trivariant phase regions. By tracing all the pseudounivariant curves detected on the boundary of a Schreinemakers diagram, all the compositionally nondegenerate phase regions of the diagram can be defined. In comparison to conventional Schreinemakers diagrams, which show only univariant curves, the advantage of this extension of the Schreinemakers projection is that it allows the determination of the compositions of phases in high variance equilibria. It is only necessary to count the number of true phases in a pseudocompound assemblage to determine the variance of the corresponding equilibrium. Such a counting procedure is used by Vertex to discriminate between equilibria of different variance.

The chemically open system $CaO–Al_2O_3–SiO_2–FeO–H_2O–CO_2–O_2$ is widely applied as a model for skarn systems and will be used to demonstrate the application of the procedures just described. To simplify this example, phase diagrams for this system were calculated with the assumptions that (1) the system is saturated with respect to SiO_2 and a fluid phase, (2) oxygen fugacity is restricted to values consistent with the magnetite-hematite phase equilibrium, (3) the total pressure is 2 kb, and (4) the system is closed with respect to FeO, Al_2O_3, and CaO. Assuming the fluid phase is essentially a binary H_2O-CO_2 mixture, the natural variables for this system are $\{T, Y^f_{CO_2}, X_{FeO}, X_{Al_2O_3}\}$, where $\{X_{FeO}, X_{Al_2O_3}\}$ define the composition of the system, and the variables $\{T, Y^f_{CO_2}\}$ may be represented on the axes of a Schreinemakers diagram.

Figure 6 shows a Schreinemakers diagram for the aforementioned system calculated with Vertex. Over the range of conditions considered, two crystalline solutions are stable, garnet (Gr_{ss}) and epidote (Zo_{ss}). Both solutions are essentially binary isomorphous solutions between ferric and aluminous endmembers and are represented by pseudocompounds specified at 10 mol percent increments of the aluminous endmember, as illustrated by the composition diagram in figure 7 and by the insets of figure 6.

The Schreinemakers diagram shown in figure 6 furnishes information on the stability of phase assemblages as a function of temperature and fluid composition. For example, the positions of the univariant curves corresponding to the phase equilibria $\{Gr_{ss}, Zo_{ss}, Hm, Cc\}$ and $\{Gr_{ss}, Zo_{ss}, An, Cc\}$ span the divariant phase region $\{Gr_{ss}, Zo_{ss}, Cc\}$. If the composition phase diagram for the system is known at any T-$Y^f_{CO_2}$ condition in the diagram, the topology of the composition diagram can be determined at all other conditions by the univariant curves. The compositions of coexistent phases in univariant equilibrium can also be

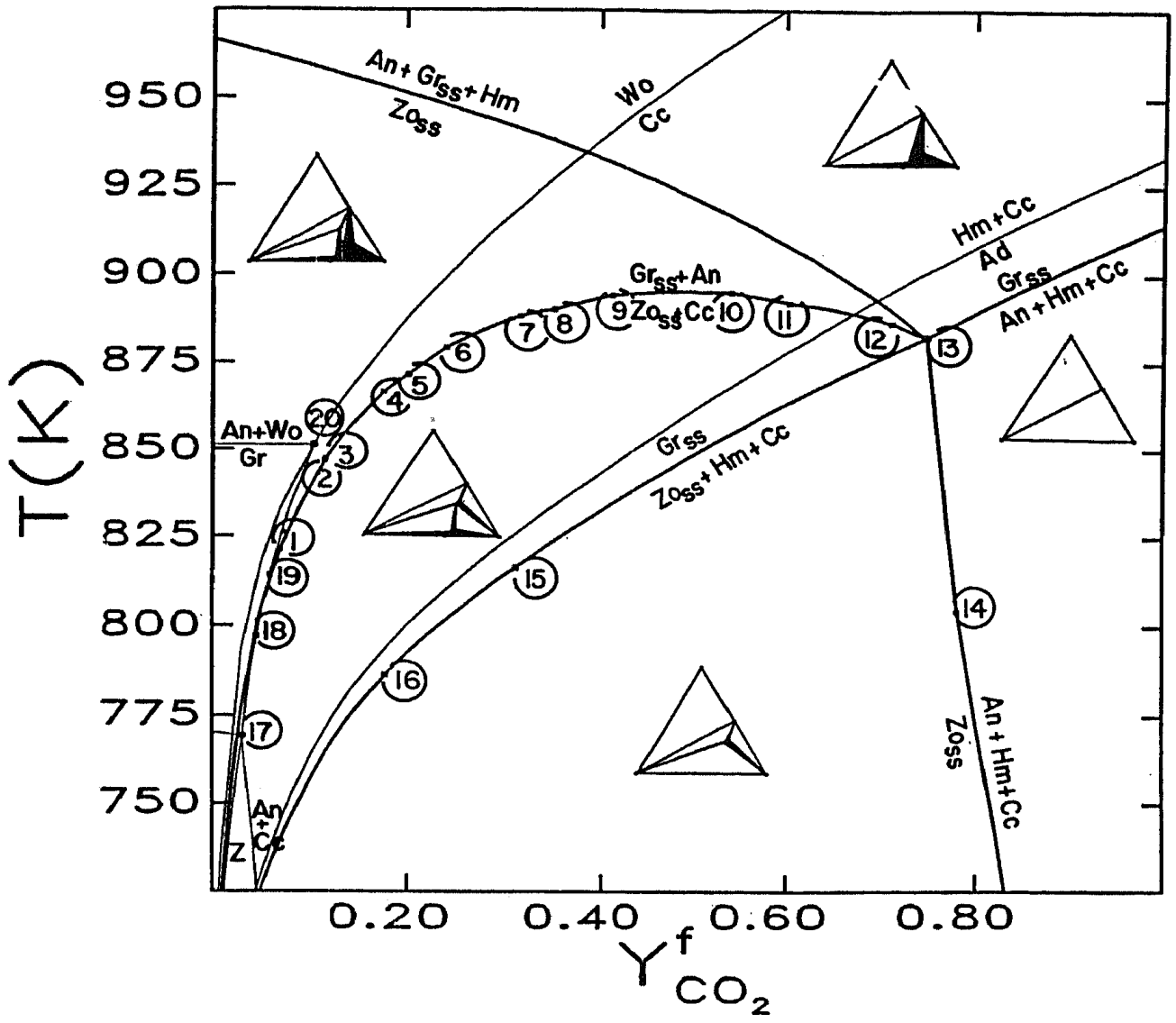

Fig. 6. Computer calculated T-$Y^f_{CO_2}$ Schreinemakers diagram for fluid and SiO_2 saturated $CaO–Al_2O_3–SiO_2–FeO–H_2O–CO_2–O_2$ with μ_{O_2} externally buffered by the magnetite-hematite equilibrium (P = 2 kb). Univariant curves are labelled by phases of the corresponding reaction; if the reaction has constant coefficients the curve is drawn by a heavy line. Composition diagrams illustrate phase compatibilities in different portions of the Schreinemakers net (invariant and divariant regions are open and filled, respectively, compare fig. 7). Invariant and pseudoinvariant assemblages are identified in table 1. Data from Helgeson and others (1978) and Connolly and Bodnar (1983).

retrieved from knowledge of the pseudoinvariant assemblages. Thus, between the pseudoinvariant points labelled 10 and 11 (fig. 6) it can be deduced from the pseudoinvariant assemblages, {Gr_{30}, Zo_{40}, Zo_{30}, An, Cc} and {Gr_{40}, Gr_{30}, Zo_{30}, An, Cc} (table 1), that epidote of composition about Zo_{35}, in equilibrium with calcite, decomposes with increasing temperature to anorthite and garnet of composition about Gr_{35}.

Quantitative information about the equilibrium compositions of coexisting phases in high variance assemblages is lost in the projection shown in figure 6. Consequently, the constraints on the composition of the system that are necessary to obtain a particular assemblage are also

TABLE 1

Phase assemblages of invariant and pseudoinvariant fields in figures 6 and 8. Assemblages marked by an asterisk are invariant in compositionally degenerate subsystems

Invariant Assemblages

(13)	Zo_{30}	+ Gr_{20}	+ Hm	+ An	+ Cc

Pseudoinvariant Assemblages

(1)	Zo_{80}	+ Zo_{70}	+ Gr_{90}	+ An	+ Cc
(2)	Zo_{70}	+ Zo_{60}	+ Gr_{90}	+ An	+ Cc
(3)	Zo_{60}	+ Gr_{90}	+ Gr_{80}	+ An	+ Cc
(4)	Zo_{60}	+ Gr_{80}	+ Gr_{70}	+ An	+ Cc
(5)	Zo_{60}	+ Zo_{50}	+ Gr_{70}	+ An	+ Cc
(6)	Zo_{50}	+ Gr_{70}	+ Gr_{60}	+ An	+ Cc
(7)	Zo_{50}	+ Gr_{60}	+ Gr_{50}	+ An	+ Cc
(8)	Zo_{50}	+ Zo_{40}	+ Gr_{50}	+ An	+ Cc
(9)	Zo_{40}	+ Gr_{50}	+ Gr_{40}	+ An	+ Cc
(10)	Zo_{40}	+ Gr_{40}	+ Gr_{30}	+ An	+ Cc
(11)	Zo_{40}	+ Zo_{30}	+ Gr_{30}	+ An	+ Cc
(12)	Zo_{30}	+ Gr_{30}	+ Gr_{20}	+ An	+ Cc
(14)	Zo_{40}	+ Zo_{30}	+ An	+ Hm	+ Cc
(15)	Zo_{30}	+ Zo_{20}	+ Gr_{20}	+ Hm	+ Cc
(16)	Zo_{20}	+ Gr_{20}	+ Gr_{10}	+ Hm	+ Cc
(17)*	Zo_{100}	+ Zo_{90}	+ Gr_{100}	+ An	+ Cc
(18)	Zo_{90}	+ Zo_{80}	+ Gr_{100}	+ An	+ Cc
(19)	Zo_{90}	+ Zo_{80}	+ Gr_{90}	+ An	+ Cc
(20)*	Gr_{100}	+ Gr_{90}	+ An	+ Wo	+ Cc
(21)	Gr_{90}	+ Gr_{80}	+ An	+ Wo	+ Cc
(22)	Gr_{80}	+ Gr_{70}	+ An	+ Wo	+ Cc
(23)	Gr_{70}	+ Gr_{60}	+ An	+ Wo	+ Cc
(24)	Zo_{50}	+ Zo_{40}	+ Gr_{60}	+ Gr_{50}	+ Cc
(25)	Zo_{40}	+ Zo_{30}	+ Gr_{40}	+ Gr_{30}	+ Cc
(26)	Zo_{60}	+ Zo_{50}	+ Gr_{80}	+ Gr_{70}	+ Cc

unspecified. As discussed previously, this information can also be calculated and drawn in Schreinemakers projections, as illustrated in figure 8. To simplify figure 8, only phase equilibria consistent with CaO saturation are shown; in this restricted context the system retains one independent compositional variable, X_{FeO} or $X_{Al_2O_3}$. The diagram in figure 8 is thus a projection of a three-dimensional section of a nine-dimensional phase diagram, whereas the diagram in figure 6 is the projection of a four-dimensional section.

The calculated phase relations shown in figures 6, 7, and 8 are dependent on the relative order in which saturation constraints are applied. The diagrams in figures 6, 7, and 8 are for systems saturated first with respect to fluid, second with respect to SiO_2, and, in figure 8, third with respect to CaO. Thus, the stable CaO-saturated phase is

wollastonite ($CaSiO_3$) at high temperatures and H_2O-rich conditions and calcite ($CaCO_3$) at low temperatures and CO_2-rich conditions (in extremely water-rich fluids, portlandite, lime, or zonotolite could be stable CaO saturated phases, but these phases were not considered in the calculation).

To understand the utility of figure 8, it may be useful to examine two-dimensional mixed-variable diagrams constructed by sectioning this diagram parallel to the temperature axis (fig. 9). These sections reveal that univariant curves in figure 8 correspond to eutectoidal and peritectoidal equilibria, and that pseudounivariant curves define the iron-aluminum fractionation of the garnet and epidote solutions. For example, the pseudounivariant curves extending from points 1 to 16, 18, 19, and 24 to 26 (points 17–19 are unlabelled in fig. 8 but can be identified with reference to fig. 6) approximately define the iron distribution between coexistent garnet and epidote. It should be emphasized that a pseudounivariant curve such as the curve which corresponds to the equilibrium:

$$Zo_{50} = Zo_{40} + An$$

does not define the limiting stability conditions of epidote solutions of

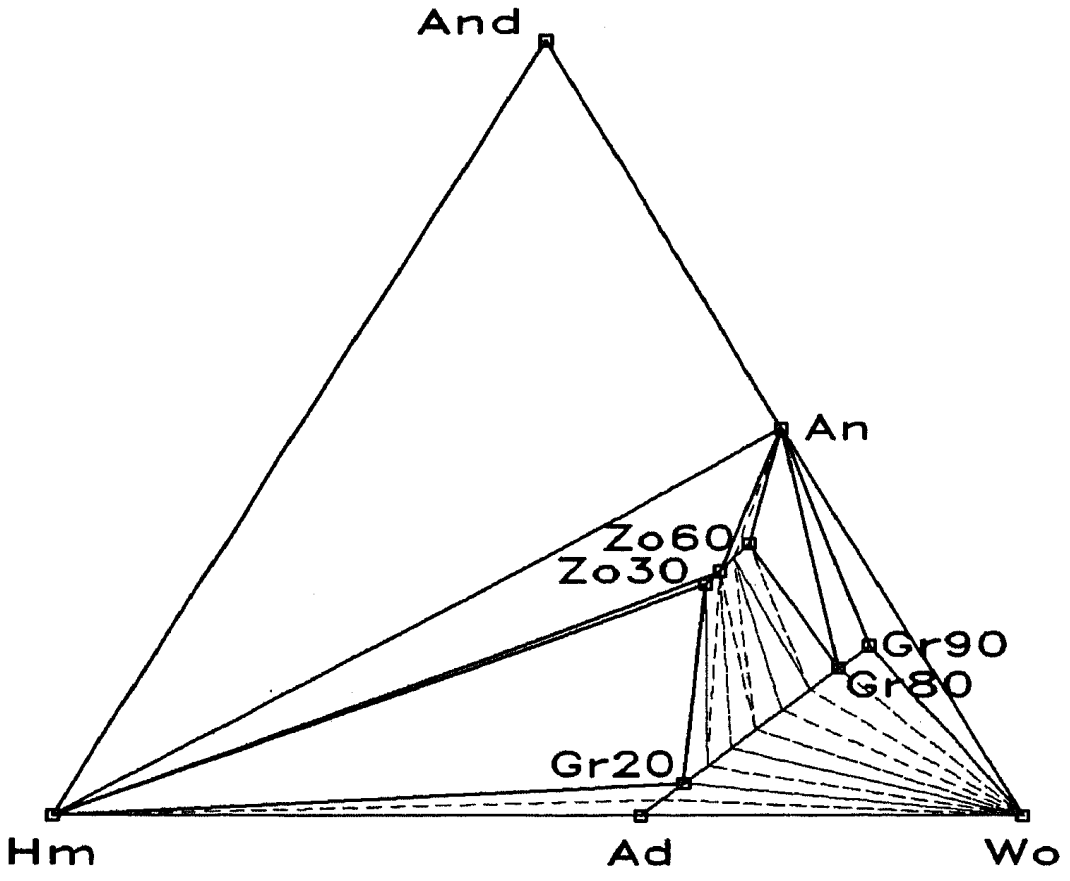

Fig. 7. Computer calculated and drafted composition diagram for the system of figure 6 at T = 875 K $Y^f_{CO_2} = 0$.

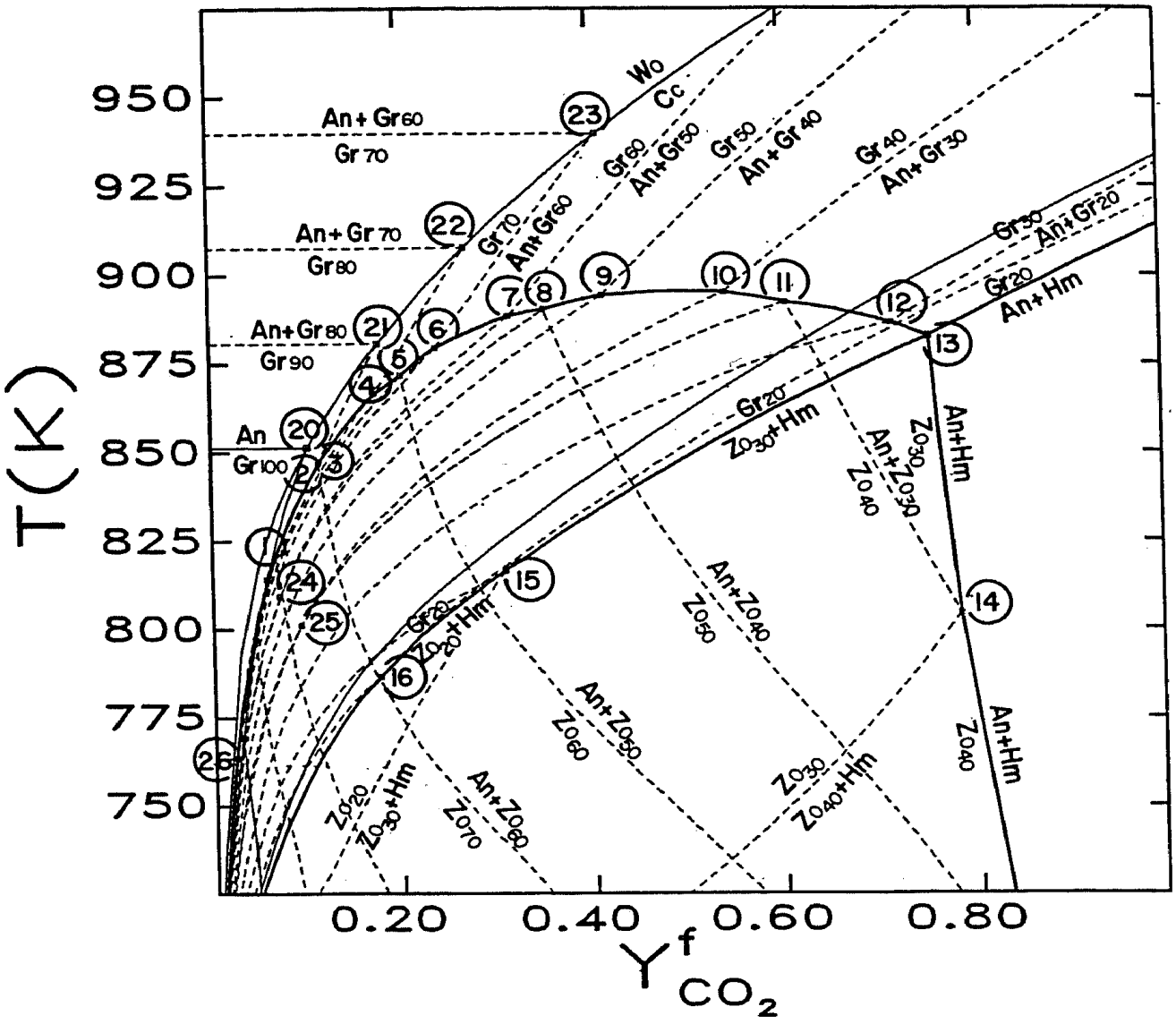

Fig. 8. Schreinemakers diagram for system of figure 6 with the added constraint of CaO saturation and showing the conditions of pseudounivariant equilibria. Unlabelled invariant and pseudoinvariant fields can be identified by comparison with figure 6.

composition Zo_{50}, rather it locates the approximate limit of stability of epidote solutions of composition Zo_{45}. The uncertainty of this approximation depends on the number of pseudocompounds used to represent a solution, the curvature of the thermodynamic surface of the solution, and the number of solutions in equilibrium. It is thus difficult to make strong statements about the accuracy of this method, but if an equilibrium involves only one solution phase, the stability field of the solution is underestimated. In contrast, when more than one solution is stable, the curvature of the thermodynamic surfaces tends to result in cancelling errors.

Two peculiar features in figures 8 and 9 deserve special mention. The more obvious is the kink in the garnet-anorthite stability field which occurs with increasing temperature (fig. 9B). This kink is the result of a singularity in the CaO-saturation surface because of the phase

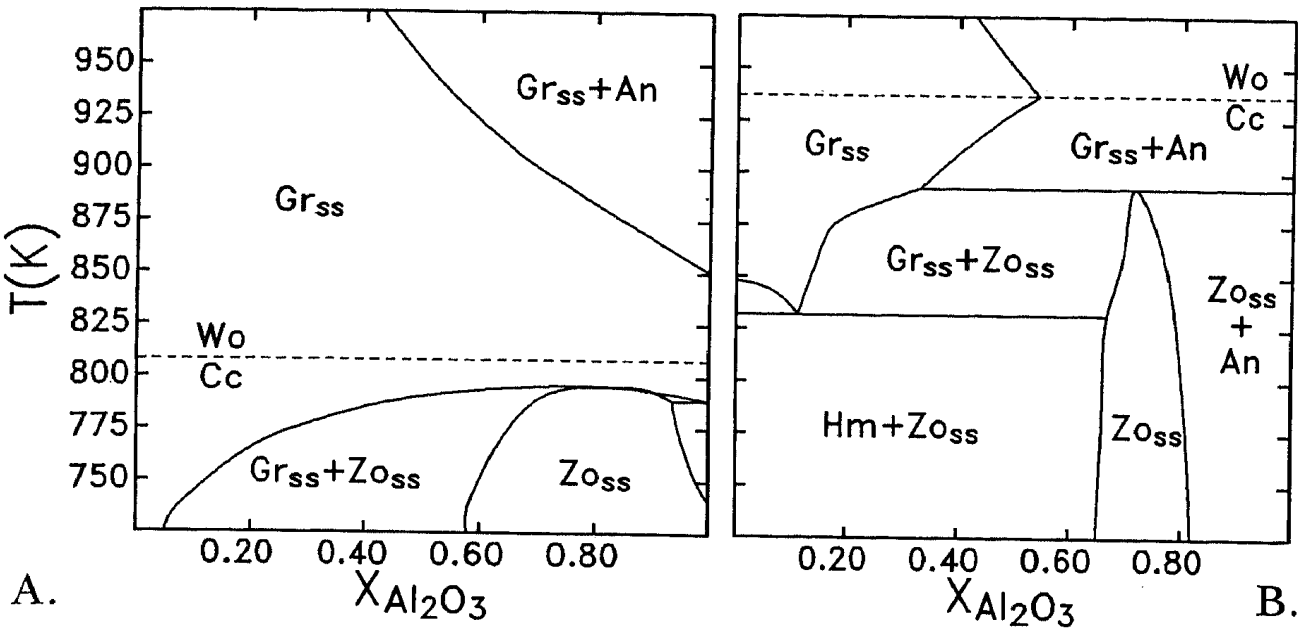

Fig. 9. Computer calculated and drafted constant $Y^f_{CO_2}$ sections of figure 8, (A) $Y^f_{CO_2} = 0.04$ mol, and (B) $Y^f_{CO_2} = 0.40$ mol.

change from calcite to wollastonite. This has the interesting implication that garnet-anorthite assemblages, which are stable in high temperature H_2O-rich environments, become unstable with decreasing temperature only to restabilize at lower temperatures. The other, more subtle, feature is observed along the univariant curve that determines the upper thermal stability of epidote (points 1-13, fig. 8). From figure 9 it is evident that the corresponding reaction is peritectoidal at high $Y^f_{CO_2}$ (fig. 9B) and in more H_2O-rich conditions becomes congruent (fig. 9A). The transition from peritectoid to congruent reaction should define a singular point, at which the peritectoidal composition of epidote becomes degenerate with that of coexistent garnet.[13] This point must also coincide with the equilibrium of a eutectoidal reaction that limits the stability of garnets more aluminous than coexistent epidote. From figure 6 or 8 (and table 1) it can be determined that the congruent reaction:

$$Zo_{70} = Gr_{90}$$

begins at point 1 {T = 812 K, $Y^f_{CO_2} = 0.068$ mol CO_2}, and from figure 8A it is evident that the eutectoidal decomposition of aluminous garnet must degenerate at a second singular point in fluids more H_2O-rich than $Y^f_{CO_2} = 0.04$ mol CO_2. However, consideration of the invariant assem-

[13]This transition does not occur with an ordered model for epidote solutions, that is, ordered epidote is always more aluminous than coexistent garnet. Although the ordered epidote model is a more appropriate natural analog than the completely disordered epidote model (Holdaway 1972; Bird and Helgeson 1981), the phase diagram for disordered epidote was presented here to illustrate the complications associated with the evaluation of singular points.

blage at point 19 {T = 814 K, $Y^f_{CO_2}$ = 0.058 mol CO_2} leads to the conclusions that the eutectoidal reaction is not represented in figures 6 and 8, and that the peritectoidal reaction that corresponds to the curve connecting points 1 and 19 (point 19 is not labelled in fig. 8) is inconsistent with the congruent epidote-garnet reaction. This kind of error is an intrinsic flaw with the pseudocompound representation and result because continuous variations are approximated by discrete changes; consequently, caution must be applied in the interpretation of singular conditions. It should be noted, however, that the error in figures 6 and 8 is important only between T = 814-801K and $Y^f_{CO_2}$ = 0.068-0.057 mol CO_2. In fact, it can be determined that in the correct topology of figures 6 and 8, point 19 should be a singular point which would occur at temperatures below the congruent reaction.

Figure 9 shows another Schreinemakers projection of the CaO–Al_2O_3–SiO_2–FeO–H_2O–O_2 phase diagram, but in this case the isothermal-isobaric water saturated phase relations are shown as a function of μ_{FeO} and μ_{O_2}. In the calculation of figures 6 to 9 pseudocompounds were used to express the free energy of solutions as a function of composition. In contrast, in the calculation of figure 10 pseudocompounds were used to obtain an expression for the free energy as a function of μ_{FeO} and μ_{O_2}.

Although the pseudoinvariant points are not labelled in figure 10, the compositions of the stable solutions can be determined given that the notations Al-Gt, Fe-Gt, and Al-Ep signify the pure aluminous and iron endmembers of the garnet and epidote solutions. Thus, the univariant curve labelled {Al-Gt, Fs, Ge, Wo} delimits the stability of garnet (Gr_{100}) with increasing μ_{FeO} at low μ_{O_2}. As this curve is traced each pseudoinvariant condition indicates a 10 mol percent shift in the iron concentration, relative to aluminum, of the garnet. In this manner it can be determined that garnet contains about 90 mol percent of the iron endmember (Ad) in the invariant equilibrium {Lm, Fs, Ge, Wo, Gt}. Along the univariant curves that define the limiting conditions of garnet stability, two pseudounivariant curves extend from each pseudoinvariant point. These curves are iron isopleths for garnets in five different divariant phase fields which can be deduced by Schreinemakers' rules. The curves with lower $d\mu_{FeO}/d\mu_{O_2}$ contour the divariant field {Gt, Wo, Fs}, whereas the curves with higher $d\mu_{FeO}/d\mu_{O_2}$ contour the fields {Gt, Ge Fs}, {Gt, Ge, Lm}, {Gt, Wo, Lm}, and {Gt, Ge, Wo}. The change in slope of the garnet field boundary has interesting implications for the stability of garnet at constant μ_{O_2} as a function of μ_{FeO}. For example, at μ_{O_2} = −750 kJ/mol and low μ_{FeO} aluminous garnet is stable; this garnet is stable to μ_{FeO} = −246 kJ/mol. As μ_{FeO} is increased beyond this condition garnet becomes metastable with respect to the assemblage {Fs, Ge, Wo}. If μ_{FeO} is increased still further to −230 kJ/mol (ferric) garnet is again stabilized. With an additional increase in μ_{FeO} to a value of −185 kJ/mol, pure ferric garnet finally decomposes to the assemblage {Lm, Fs, Ge}. Because figure 10 represents a projection of a four-dimensional diagram, these phase relations would be virtually impossible to predict on

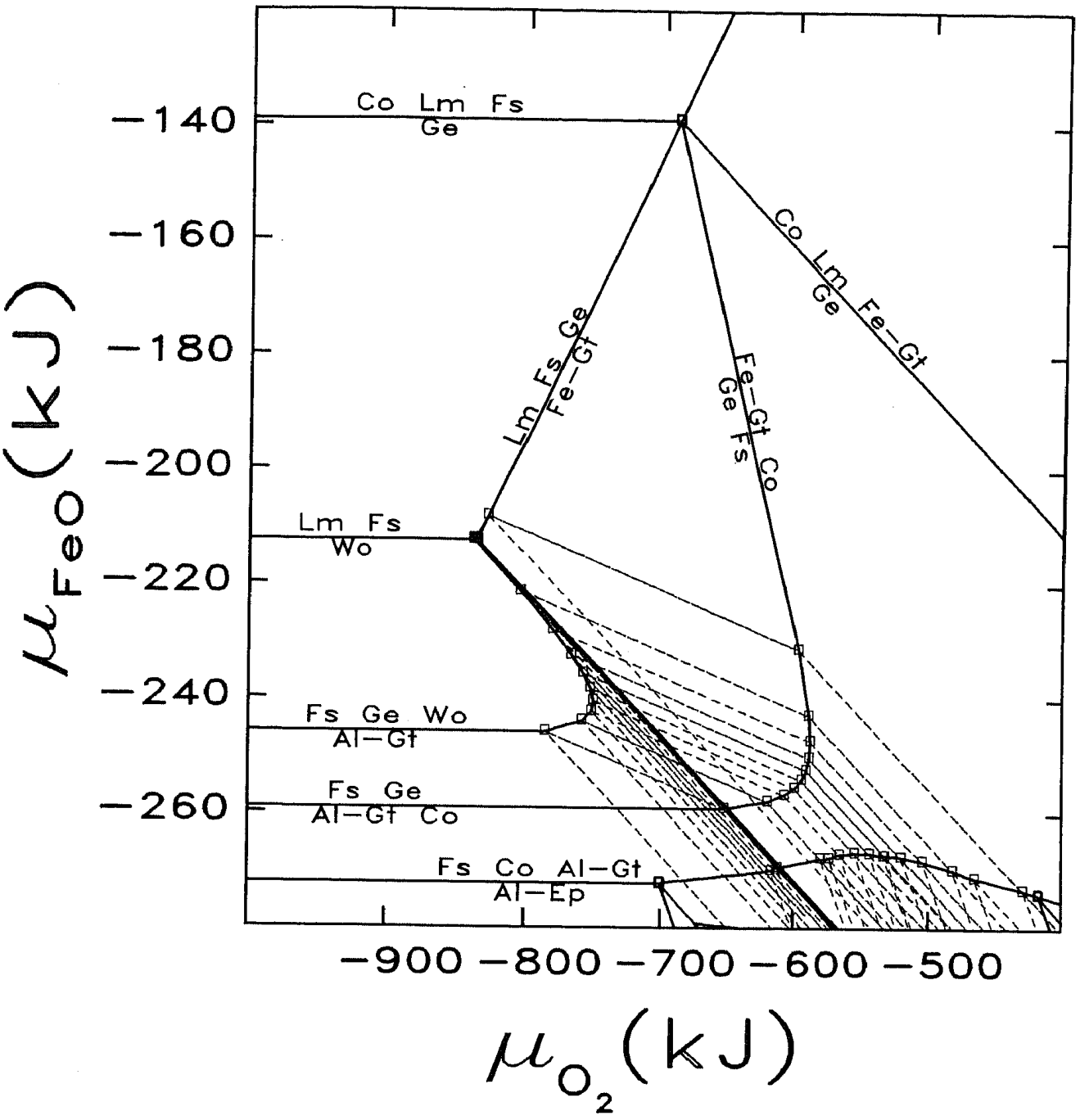

Fig. 10. Computer calculated and drafted Schreinemakers diagram for the isobaric (P = 2 kb)-isothermal (T = 875 K) water saturated system $CaO–Al_2O–SiO_2–FeO–H_2O–O_2$. Univariant and pseudounivariant curves are drawn, respectively, by heavy solid lines and light dashed lines. Pseudounivariant curves are drawn twice by the graphics device, consequently in some cases dashed line patterns appear continuous. Data from Helgeson and others (1978) and Connolly and Bodnar (1983).

an a priori basis. For simplicity the aluminosilicates (andalusite) and solution of ferrous garnet were not considered in the calculation of figure 10.

High variance phase fields.—It is often useful to define a specific phase field as a function of potentials. This information is contained in Schreinemakers diagrams, but the extraction of the information is not

always simple. As an alternative, the projection of high variance phase fields may be calculated directly. In Vertex this is done by determining the Ω-X plane defined by the assemblage in question. The stability of the assemblage can then be tested by condition (23) within a specified two-dimensional potential coordinate frame. If the field is bounded within the coordinate frame, the boundary can be associated with a univariant or pseudounivariant equilibrium. Therefore, if one bounding condition can be identified by an incremental search, then the remaining conditions can be traced rapidly by the techniques employed to establish Schreinemakers nets, as previously described. Optionally, the compositions of coexistent phases in a high variance phase region can be specified, in which case the program determines only the portion of the equilibrium phase field consistent with the specified compositions.

Figure 11 shows isobaric T-$Y^f_{CO_2}$ sections in which the divariant phase field {Gr, An, Cc} is outlined for the chemical system CaO–Al_2O_3–SiO_2–H_2O–CO_2. The calculations were done with two different sources of thermochemical data (Helgeson and others, 1978; Robinson and others, 1983) and reveal substantial discrepancies between the data compilations. This example also demonstrates the utility of coupling

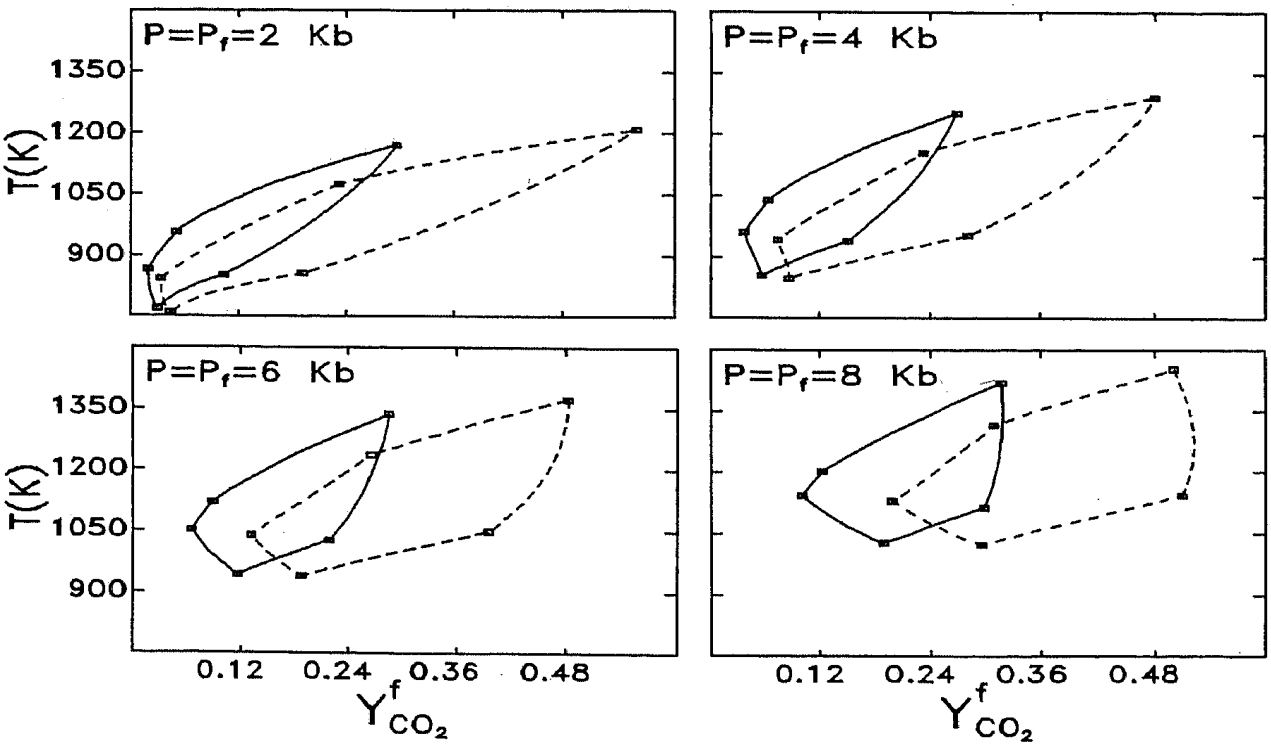

Fig. 11. Computer calculated and drafted projections of isobaric T-Y_{CO_2} sections showing the divariant phase field {Gr, An, Cc} in the chemical system CaO–Al_2O_3–SiO_2–H_2O–CO_2. Invariant fields (indicated by square symbols) are defined by the assemblages {An, Gr, Cc, Q, Zo}, {An, Gr, Cc, Q, Wo}, {An, Gr, Cc, Ge, Wo}, {An, Gr, Cc, Ge, Co}, and {An, Gr, Cc, Zo, Co}, counterclockwise from lowest temperatures. Solid and dashed curves were calculated with data from Helgeson and others (1978) and Robinson and others (1983), respectively.

phase diagram calculating programs with computer graphics to facilitate the comparison of data and other computational options.

Frequently it is important to define the range of conditions a set of minerals will have on certain prescribed equilibrium compositions. In this case it is necessary to determine only the portion of a high variance phase field consistent with the specified compositions. Calculations of this type are familiar in the context of geothermobarometry, although in geothermobarometry it is usually presumed that the observed assemblage is in stable equilibrium. This a priori assumption may be inconsistent with the thermodynamic models being employed; in contrast stability calculations with Vertex determine internally consistent conditions. For such calculations it is necessary to associate an "uncertainty" with the composition of at least one phase; this uncertainty is then used to define a set of pseudocompounds from which pseudodivariant assemblages can be generated. The stability of all possible assemblages generated in this manner can then be determined. The "uncertainty" is arbitrary and can be made to approach zero if desired. Figure 12 illustrates a calculation to solve a problem of this type for the mineral assemblage $\{Mu_{94.2+/-.8}, Ab_{91.2+/-.8}, Q\}$, in equilibrium with water, as a function of pressure and temperature. This assemblage is part of the trivariant muscovite-albite phase field in the silica and water saturated chemical system Na_2O–K_2O–Al_2O_3–SiO_2–H_2O. In this system the stable conditions for $\{Mu_{94.2+/-.8}, Ab_{91.2+/-.8}, Q\}$ are restricted to a band of temperatures of about 30 K bounded by two dashed curves superimposed on the Schreinemakers diagram in figure 12A. These curves are defined by the reaction (fig. 12B):

$$Ab_{93.6} + Mu_{94.8} = Ab_{92.2} + Mu_{93.6}$$

at low temperature, and, at high temperature by the reaction:

$$Ab_{92.2} + Mu_{93.6} = Ab_{90.4} + Mu_{92.1}.$$

An interesting feature of figure 12 is that within this band there is a wedge-shaped region, which tapers out at high pressure, of conditions for which the specified assemblage is metastable with respect to muscovite-orthoclase assemblages. The existence of this wedge reflects the fact that Na-solution increases with pressure more rapidly in the muscovite phase than in the albite phase for the range of conditions shown.

For the calculation of figure 12 each solution was represented by twenty compounds specified by a logarithmic subdivision scheme useful for solutions that exhibit immiscibility (Connolly and Kerrick, 1987). The muscovite-feldspar phase fields are poorly constrained by the univariant phase fields in figure 12A; however, the projection of the pseudounivariant fields for this problem involves 342 curves and is virtually indecipherable. Calculation of the Na_2O–K_2O–Al_2O_3–SiO_2–H_2O Schreinemakers diagram in figure 12 required a total of 15 sec of CPU time. Comparison with the efforts required in previous calcula-

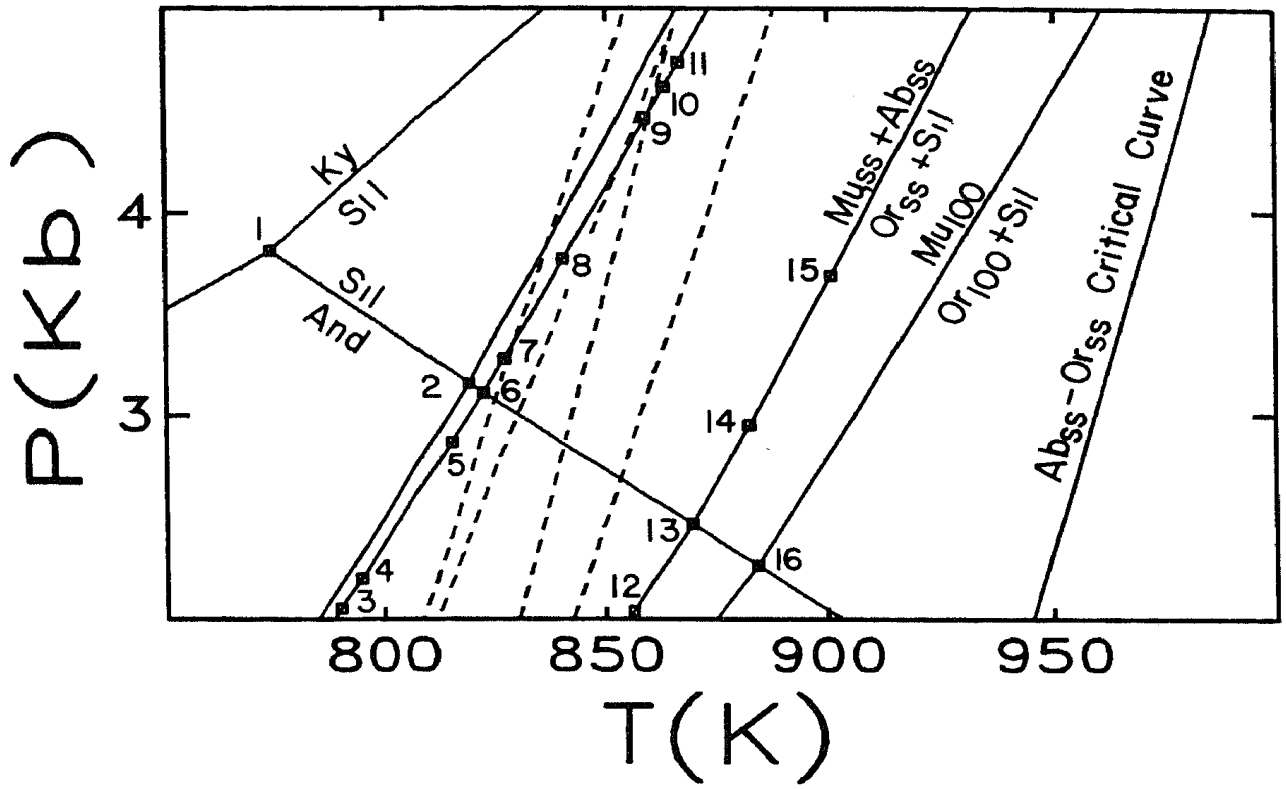

A.

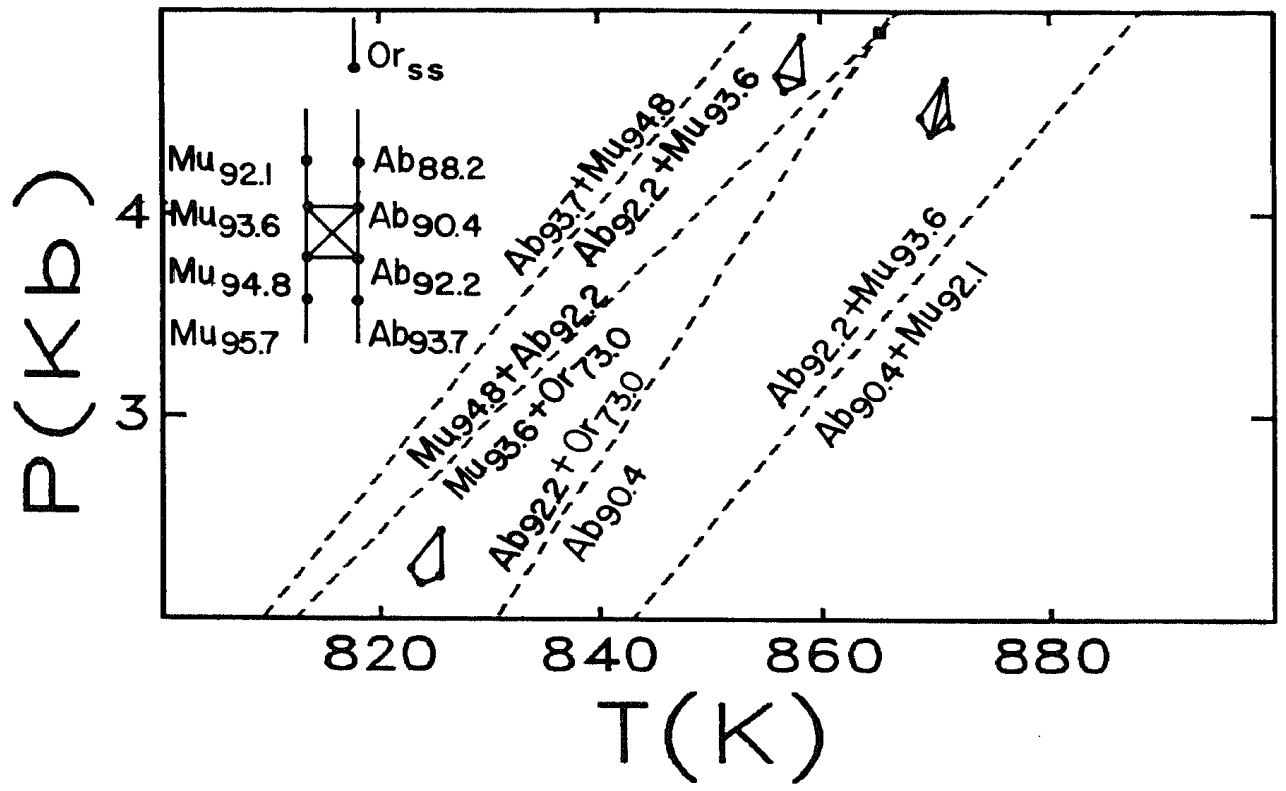

B.

Fig. 12(A) Computer calculated Schreinemakers projection of univariant phase fields (solid curves) in water and silica saturated Na_2O–K_2O–Al_2O_3–SiO_2–H_2O systems. Phase assemblages can be determined from invariant and pseudoinvariant points identified in table 2. Stable conditions for $\{Mu_{94.2+/-.8}, Ab_{91.2+/-.8}, Q\}$, as discussed in the text, are bounded by the dashed curves. (B)Detail showing pseudounivariant fields and schematic chemographic relations. Data from Helgeson and others (1978), excess functions for mica and feldspar from Chatterjee and Froese (1975) and Thompson and Waldbaum (1972), respectively, and water properties from Kerrick and Jacobs (1981).

TABLE 2

Phase assemblages of invariant and pseudoinvariant fields in figures 11. Assemblages marked by an asterisk are invariant in compositionally degenerate subsystems

Invariant Assemblages

(1a)	And	+ Ky	+ Sil	+ Mu_{ss}	
(1b)	And	+ Ky	+ Sil	+ Pa_{ss}	
(6)	$Pa_{90.4}$	+ $Ab_{98.2}$	+ $Mu_{82.1}$	+ And	+ Sil
(13)	$Mu_{92.1}$	+ $Ab_{88.2}$	+ $Or_{66.8}$	+ And	+ Sil

Pseudoinvariant Assemblages

(2)*	Pa_{100}	+ Ab_{100}	+ $Ab_{98.9}$	+ And	+ Sil
(3)	$Pa_{93.7}$	+ $Pa_{92.2}$	+ $Ab_{98.5}$	+ $Mu_{82.1}$	+ And
(4)	$Pa_{92.2}$	+ $Ab_{98.5}$	+ $Ab_{98.2}$	+ $Mu_{82.1}$	+ And
(5)	$Pa_{92.2}$	+ $Pa_{90.4}$	+ $Ab_{98.2}$	+ $Mu_{82.1}$	+ And
(7)	$Pa_{90.4}$	+ $Ab_{98.2}$	+ $Ab_{97.8}$	+ $Mu_{82.1}$	+ Sil
(8)	$Pa_{90.4}$	+ $Pa_{88.2}$	+ $Ab_{97.8}$	+ $Mu_{82.1}$	+ Sil
(9)	$Pa_{88.2}$	+ $Ab_{97.8}$	+ $Mu_{82.1}$	+ $Mu_{78.0}$	+ Sil
(10)	$Pa_{88.2}$	+ $Ab_{97.8}$	+ $Ab_{97.3}$	+ $Mu_{78.0}$	+ Sil
(11)	$Pa_{88.2}$	+ $Pa_{85.5}$	+ $Ab_{97.3}$	+ $Mu_{78.0}$	+ Sil
(12)	$Mu_{92.1}$	+ $Ab_{85.5}$	+ $Ab_{88.2}$	+ $Or_{66.8}$	+ And
(14)	$Mu_{92.1}$	+ $Ab_{88.2}$	+ $Or_{66.8}$	+ $Or_{59.3}$	+ Sil
(15)	$Mu_{92.1}$	+ $Ab_{88.2}$	+ $Ab_{85.5}$	+ $Or_{59.3}$	+ Sil
(16)*	$Mu_{92.1}$	+ Or_{100}	+ $Or_{98.9}$	+ And	+ Sil

tions of this diagram (Thompson, 1974; Chatterjee and Froese, 1975) gives ample justification for the development of completely automated procedures.

DETAILS OF THE PROGRAM

Vertex has been coded as a FORTRAN computer program. To make calculations with Vertex the user must specify the compositional variables, potential variables, constraints, and a data source. The program then sorts through the data source to identify possible phases, determines the appropriate state function, subdivides solution phases into pseudocompounds, and does the requested calculation. A number of thermodynamic data bases have been formatted for use with Vertex, these include Helgeson and others, (1978), Haas, Robinson, and Hemingway (1981), Robinson and others (1983), Powell and Holland (1985, updated in 1989), and Berman (1988). Although detailed documentation of the options supported with Vertex is not warranted here, some aspects of the data and physical requirements relevant to the assessment of the capabilities of Vertex and are addressed.

Vertex is currently structured for calculations with up to seven thermodynamic components, three saturated or constrained components, four potential variables, and one saturated phase. In this configu-

ration, with dimensioning for 1000 pseudocompounds, the complete program requires a region of memory of 855 kbytes, of which 625 kbytes are required for array storage. However, the program can be overlaid, with little loss of computational efficiency, in which case memory requirements are reduced to 275 kbytes. The program has been compiled and run successfully on Sun, IBM, DEC, CDC, and MacIntosh (PC) computers. Graphics programs have been written for the following commercial software packages: Precision Visuals (DI-3000), SunCore, SunPhigs, and Evans and Sutherland (MPS).

Thermodynamic Input

In theory it should be possible to make the procedures in Vertex completely symmetric with respect to the choice of compositional and potential variables selected for a given calculation. This would require that the state functions specified in the input to the program be expressed completely as a function of compositional or extensive variables, for example $S = f(U, V, n_1, \ldots, n_k)$. However, this is impractical because the vast majority of calculations are done with the Gibbs energy or derivatives of it obtained by interchanging extensities with potentials. State functions are, therefore, invariably tabulated as a function of the natural variables of the Gibbs energy $\{P, T, n_1, \ldots, n_k\}$. Consequently, to facilitate the use of Vertex, input is structured around the conventional functional form of the Gibbs energy.

Thermodynamic data is read from two separate files, one of these files contains data on chemical compounds, and the other contains other data on chemical solutions. Data for phases from more than one source may be stored in a file; this allows rapid comparison of the different data sources during a single execution of the program.

Compound phases.—The data for chemical compounds consists of isobaric heat capacity and volumetric functions, standard state parameters, and molar stoichiometric coefficients. The analytic forms of the heat capacity and volumetric functions currently in use are:

$$C_p^m = a + bT + c/T^2 + dT^2 + e/T^{1/2} + f/T + gT^3 \qquad (29)$$

and

$$V^m = h + iT + jT^2 + k\,[\exp(T/c_1)] + lP + mP^2 + n[\exp(P/c_2)] \qquad (30)$$

where $\{a, \ldots, n\}$ are parameters for each compound, and c_1 and c_2 are constants (compare, Robinson and others, 1983). These functions are integrated with the standard state parameters, by the program, to obtain a null reference state expression of the form:

$$\begin{aligned} G^m = {} & g_1 + g_2T + g_3P + g_4T \ln T + g_5T^2 \\ & + g_6/T + g_7T^3 + g_8T^{1/2} + g_9 \ln T \\ & + g_{10}/T^2 + g_{11}PT + g_{12} \exp(T/c_1) + g_{13}P^2 \\ & + g_{14} \exp(P/c_2) + g_{15}P^3 + g_{16}PT^2 \end{aligned} \qquad (31)$$

where $\{g_1 - g_{16}\}$ are parameters for each compound.

Temperature dependent ordering and lambda transitions are treated by the methods described by Helgeson and others (1978) and Berman and Brown (1985; also Berman, 1988) which are adequate for most oxides. The more complex functions used to describe ordering in metallic elements and alloys (Hillert 1985b) are not currently supported, but appropriate modifications could easily be made to allow them.

Solution phases.—The data for chemical solutions describe the analytic form of the excess Gibbs energy function for each phase, the parameters for this function, and codes that indicate the nature of the scheme to be used to subdivide the chemical solutions into pseudocompounds. In current versions of Vertex, chemical solutions must be identified by name in the input to the program. For Vertex it is assumed that chemical solutions can be defined in terms of stoichiometric endmembers. The Gibbs energy of each solution can, thus, be written:

$$G_{sol} = G_{mix} - TS_{ideal} + G_{excess}. \tag{32}$$

In eq (32), S_{ideal} is the ideal configurational entropy consistent with a simple (single site) or multisite model for the solution; for simple models, G_{mix} is the Gibbs energy of a mechanical mixture of the endmember compounds with the same chemical composition as the solution, and in multisite models G_{mix} is computed by the Bragg-Williams summation for nearest neighbor interactions (Wood and Nicholls, 1978); and G_{excess} is computed by the polynomial expansion:

$$G_{excess} = \sum_{k=1}^{s} W_k \left(\prod_{m=1}^{t} Z_{k(m)} \right), \tag{33}$$

where k indexes the s terms in the expansion, and $Z_{k(m)}$ represents atomic or molecular site fractions. The site fractions $\{Z_{k(1)}, \ldots, Z_{k(t)}\}$ which appear in each of the s terms in eq (33) are specified for each solution in the input to Vertex. The only restriction on eq (33) is that the functional dependence of the parameters, $W_k = f(P, T)$, must have the same form as eq (31). The reason for this requirement is that after chemical solutions have been subdivided into pseudocompounds, the Gibbs energy of the pseudocompounds can be expressed by eq (31), regardless of the actual models used to express the excess properties of solutions. By mathematical manipulation, it is possible to accommodate a wide variety of solution models with eqs (31) and (33).

After the Gibbs energy functions have been determined for each chemical pseudocompound, the free energy function, Ω, appropriate for the requested calculation is then derived by Legendre transformation. Transformations of the form $n_j \rightarrow \mu_j$ are trivial because a compound in $\{n_1, \ldots, n_k\}$ space will be a compound in any subspace. In contrast, transformations of the form $T \rightarrow S$ will transform a compound in $\{n_1, \ldots, n_k\}$ space into a solution in $\{S, n_1, \ldots, n_k\}$ space, because $S = f(P, T)$ by eq (29). It is, therefore, necessary to subdivide each solution generated by such a transformation into pseudocompounds. It is noteworthy that $n_j \rightarrow \mu_j$ transformations may transform a chemical solution into a

compound. To express $n_j = f(\mu_j)$ in such cases, a single true compound may be represented by a number of pseudocompounds. The number of compounds generated by subdivision may become very large for complex solutions, and this is the primary limitation of the applicability of Vertex. Computations have been done for quaternary thermodynamic solutions with accuracy comparable to the calculations shown in figures 5 to 9 with no deterioration in computational efficiency (<20s CPU time). However, higher order solutions may begin to tax the computational resources available to most users.

Saturated phases.—The thermodynamic equations of state for saturated phases of variable composition must be defined within a subprogram. At present, subprograms are supplied for the evaluation of fluid mixtures by the equations of state described by Holloway (1977), Kerrick and Jacobs (1981), and Saxena and Fei (1988); additionally, several hybrid equations of state, evaluated as described by Connolly and Bodnar (1983), are included. Bottinga and Richet's (1981) equation of state for pure CO_2 is also available. Given the set of parameters $\{Y^i_j, \theta_{c+1}, \theta_{c+2}, \ldots\}$, where Y^i_1 defines the composition of the saturated phase with respect to two extensive quantities $\{\psi_1, \psi_2\}$, the subprogram returns the potentials $\{\theta_1, \theta_2\}$. It is of course possible to hold Y^i_1 constant during a calculation. Calculations can be done as a function of only one compositional variable of a saturated phase at a time, although there is no limit to the total number of components in the phase.

DISCUSSION AND SUMMARY

Thermodynamics has a canonical form, and therefore phase diagrams, which are the geometric realizations of thermodynamic properties, also have a canonical basis. This leads to the conclusion that phase diagram calculations with different potentials or compositional variables are minor variations on a major computational theme. The generalized concepts of components and composition were introduced to draw attention to these basic similarities and to provide an efficient and, it is hoped, unambiguous means of describing phase diagram calculations. For this purpose, it is sufficient to associate a component with each independent extensive computational variable. No physicochemical significance for this association is ascribed with reference to phase diagrams. However, from a theoretical perspective components are associated with those attributes of a physicochemical system independent of both internal and environmental processes. The recognition of this association simplifies both the selection and interpretation of phase diagram representations.

The Vertex program has been designed to take advantage of the canonical nature of phase diagram calculations. The result is that the program is relatively compact and requires only the parameterization of one thermodynamic state function as input ($G^i = f(P, T, n^i_1, \ldots, n^i_k)$, $i = 1, \ldots, \pi$), yet it can be used to calculate a wide variety of phase diagrams. The strategy of the program avoids the practical limits

encountered with brute force combinatorial algorithms. As a result Vertex is unique in that it provides a means for completely automated calculation of multivariable phase diagrams for systems with up to seven components as a function of both composition and two potentials. The information in such multidimensional diagrams can be extracted by sectioning and with Schreinemakers projections. Schreinemakers diagrams conventionally show only univariant and invariant phase fields; accordingly, previous strategies for calculating such diagrams have been designed solely for the definition of these fields. However, in many cases the characteristics of high variance fields are important, and because Vertex may be used to calculate these fields it is possible to obtain a virtually complete phase diagram representation with Schreinemakers projections. This is accomplished by projecting the loci of conditions at which the phases of a high variance equilibrium have prespecified compositions.

For multivariable calculations it is to be expected that effective strategies will compromise between the need for efficiency and the sophistication that can be achieved for an individual equilibrium calculation. The feasibility of the strategy of Vertex results from such a compromise, which is the approximate representation of solution phases by pseudocompounds. Although such an approximation might at first appear simplistic, it is particularly well suited for computer automation and results in a robust and efficient program. With this approximation, accuracy comparable to that of numerically exact techniques, but at a fraction of the cost, can be achieved for systems with binary and ternary solutions. The utility of the pseudocompound approximation deteriorates for higher order solutions because of practical limitations. For this reason Vertex is not intended to supplant numerically exact procedures; rather, it is expected that in some cases Vertex will provide initial refinements for more sophisticated and time consuming calculations. The approximation used in Vertex for solution phases is not an inherent limitation of the strategy, and this strategy could be coupled with the numerically exact techniques described by Hillert (1981a,b) and Lukas and others (1982). However, for many purposes, particularly in oxide systems, the approximation is quite accurate and offers the advantage of certain representations that would be otherwise impractical. The approximation of solutions by pseudocompounds is certainly not new, and such an approximation could serve within other programs. The success of Vertex is therefore not the direct result of the approximation; but instead, it is the result of the development of an efficient strategy for calculating composition diagrams with the approximation.

ACKNOWLEDGMENTS

The project that led to this paper was suggested and directed by Derrill M. Kerrick, to whom the author is indebted for both advice and support. The penultimate version of this paper received a particularly thorough and useful review by Volkmar Trommsdorff. Thoughtful

reviews by Rainer Abart, Stefano Poli, David H. Eggler, Stephan I. Usdansky, James H. Stout, Peter Deines, and Karl Spear all improved this paper. Kurt Bucher-Nurminen's interest in (and patience with) Vertex provided the much-needed impetus for the final revisions of this paper. This work was done while the author was the recipient of a generous fellowship from the Owens Corning Fiberglas Corporation. Computer funds provided by The Pennsylvania State University and financial support from the Earth Sciences Section of the National Science Foundation (NSF Grant EAR-8307682 to D. M. Kerrick) are gratefully acknowledged.

References

Berman, R. G., 1988, Internally consistent thermodynamic data for minerals in the system Na_2O-K_2O-CaO-MgO-FeO-Fe_2O_3-SiO_2-Ti O_2-H_2O-CO_2; Journal of Petrology, v. 29, p. 445–552.

Berman, R. G., and Brown, T. H., 1984, A thermodynamic model for multicomponent melts: Geochimica et Cosmochimica Acta v. 48, p. 661–678.

———— 1985, Heat capacity of minerals in the system Na_2O-K_2O-CaO-MgO-FeO-Fe_2O_3-SiO_2-TiO_2-H_2O-CO_2: representation, estimation, and high temperature extrapolation: Contributions to Mineralogy and Petrology, v. 89, p. 168–183.

Bird, D. K., and Helgeson, H. C., 1981, Chemical interaction of aqueous solutions with epidote-feldspar mineral assemblages in geologic systems. I. Thermodynamic analysis of phase relations in the system CaO-Al_2O_3-FeO-Fe_2O_3-SiO_2-H_2O-C O_2: American Journal of Science, v. 280, p. 907–941.

Born, M., 1964, Natural philosophy of cause and chance: New York, Dover Publications, Inc., 355 p.

Bottinga, Y., and Richet, P., 1981, High pressure and temperature equation of state and calculation of the thermodynamic properties of gaseous carbon dioxide: American Journal of Science, v. 281, p. 615–660.

Bowen, N. L., 1940, Progressive metamorphism of siliceous limestone and dolomite: Journal of Geology, v. 48, p. 225–274.

Brown, T. H., and Skinner, B. J., 1974, Theoretical prediction of equilibrium phase assemblages in multicomponent systems: American Journal of Science, v. 274, p. 961–986.

Buchdahl, H. A., 1966, The concepts of classical thermodynamics: Cambridge, Cambridge University Press, 223 p.

Chatterjee, N. D., and Froese, E., 1975, A thermodynamic study of the pseudobinary join muscovite-paragonite in the system $KAlSi_3O_8$-$NaAlSi_3O_8$-Al_2O_3-SiO_2-H_2O: American Mineralogist, v. 60, p. 985–993.

Connolly, J. A. D., ms, 1988, Calculation of multivariable phase diagrams: A computer strategy based on generalized thermodynamics: Ph. D. thesis, The Pennsylvania State University, 105 p.

Connolly, J. A. D. and Bodnar, R. J., 1983, A modified Redlich-Kwong equation of state for H_2O-CO_2 mixtures: Application to fluid inclusion studies [abs.]: EOS, v. 64, p. 350.

Connolly, J. A. D., and Kerrick, D. M., 1987, An algorithm and computer program for calculating composition diagrams: CALPHAD, v. 11, p. 1–54.

———— 1984, VERTEX: A computer algorithm for the calculation of stable phase assemblages and Schreinemakers-type phase diagrams (abs): EOS, v. 65, p. 287.

Conte, S. C., and de Boor C., 1980, Elementary numerical analysis: New York, McGraw-Hill Co., 386 p.

DeCapitani, C., and Brown, T. H., 1987, The computation of chemical equilibrium in complex systems containing non-ideal solutions: Geochimica et Cosmochimica Acta, v. 51, p. 2639–2652.

Day, H. W., Chernovsky, J. V., and Kumin H. H., 1985, Equilibria in the system MgO-SiO_2-H_2O; a thermodynamic analysis: American Mineralogist, v. 70, p. 237–248.

Eriksson, G., 1971, Thermodynamic studies of high temperature equilibria: Acta Chemica Scandavia, v. 25, p. 2651–2658.

Eriksson, G., and Hack, K., 1984, Calculation of phase equilibria in multicomponent alloy systems using a specially adapted version of the program 'SOLGASMIX'; CALPHAD, v. 8, p. 15–24.

Fujii, T., 1977, The configuration of the univariant curves and their metastable extensions around an invariant point on a P-T diagram: Journal of Geology, v. 85, p. 571–589.
Gibbs, J. W., 1957, The collected works of J. Willard Gibbs, volume I, Thermodynamics: New Haven, Yale University Press, 371 p.
Gillespie, L. J., and Coe, J. R., Jr., 1933, The heat of expansion of a gas of varying mass: Journal of Chemical Physics, v. 9, p. 103–113.
Gokcen, N. A., 1975, Thermodynamics, Hawthorne, Techscience Inc., 460 p.
Haas, J. L., Robinson, G. R., Jr., and Hemingway, B. S., 1981, Thermodynamic tabulations for selected phases in the system system CaO-Al_2O_3-SiO_2-H_2O at 101.325 kPa (1 atm) between 273.15 and 1800 K: Journal of Physical Chemistry Reference Data, v. 10, p. 575–669.
Helgeson, H. C., Delany, J. M., Nesbitt, H. W., and Bird, D. K., 1978, Summary and critique of the thermodynamic properties of rock forming minerals: American Journal of Science, v. 278-A, p. 1–229.
Hillert, M., 1981a, Some viewpoints on the use of a computer for calculating phase diagrams: Physica, v. 103B, p. 31–40.
———— 1981b, A discussion of methods of calculating phase diagrams: Bulletin of Alloy Phase Diagrams, v. 2, p. 265–268.
———— 1982, Predictions of the slopes of phase boundaries: Bulletin of Alloy Phase Diagrams, v. 3, p. 4–8.
———— 1985a, Principles of phase diagrams: International Metals Reviews, v. 30, p. 45–67.
———— 1985b, Thermodynamic modeling of phase diagrams—a call for increased generality: TRITA-MAC-0276, 14 p.
Holdaway, M. J., 1965, Thermal stability of aluminum-iron epidote as a function of f_{O_2} and iron content: Contributions to Mineralogy and Petrology, v. 36, p. 307–340.
Holland, T. J. B., and Powell, R., 1985, An internally consistent thermodynamic dataset with uncertainties and correlations: Data and results: Journal of Metamorphic Petrology, v. 3, p. 343–370.
Holloway, J. R., 1977, Fugacity and activity of molecular species in supercritical fluids, *in* Fraser, D., ed., Thermodynamics in geology: Boston, D. Reidel Pub. Co., p. 161–181.
Hudson, J. F. P., 1959, Piecewise linear topology: New York, W.A. Benjamin, Inc., 282 p.
Kaufman, L., and Bernstein, H., 1970, Computer calculation of phase diagrams with special reference to refractory metals: New York, Academic Press, 384 p.
Kerrick, D. M., and Jacobs, G. K., 1981, A modified Redlich-Kwong equation for H_2O, CO_2, and H_2O-CO_2 mixtures at elevated temperatures and pressures: American Journal of Science, v. 281, p. 735–767.
Korzhinskii, D. S., 1959, Physicochemical basis of the analysis of the paragenesis of minerals: New York, Consultants Bureau, Inc., 142 p.
Landsberg, P. T., 1956, Foundations of thermodynamics: Review of Modern Physics, v. 28, p. 363–392.
Lin, P.-L., Pelton, A. D., Bale, C. W., Thompson, W. T., 1980, An interactive program for calculating ternary phase diagrams: CALPHAD, v. 4, p. 47–60.
London, F., 1954, Superfluids, v. II: New York, Wiley, 217 p.
Lukas, H. L., Weiss, J., and Henig, E.-Th., 1982, Strategies for the calculation of phase diagrams: CALPHAD, v. 6, p. 229–251.
Nuamov, G. B., Ryzhenko, B. N., and Khodakovsky, I. L., 1971, Handbook of thermodynamic data: (translation) U.S. Geological Survey Report WRD-74-001, 328 p.
Palatnik, L. S., and Landau, A. I., 1964, Phase equilibria in multicomponent systems: New York, Holt, Rinehart, and Winston, Inc., 454 p.
Perkins, E. H., Brown, T. H., and Berman R. G., 1986, PTX-SYSTEM: Three programs for calculation of pressure-temperature-composition phase diagrams: Computers and Geosciences, v. 12, p. 749–755.
Rey de Luna, A., and Zamora, M., 1986a, Canonical formalism in equilibrium thermodynamics: Journal of Chemical Physics, v. 84, p. 4612–4618.
————1986b, Canonical formalism in equilibrium thermodynamics, II. Homogeneity, stability, and generalized Maxwell relations: Journal of Chemical Physics, v. 84, p. 4612–4618.
Rice, D. R., and Ferry, J. M., 1982, Buffering, infiltration and control of intensive variables during metamorphism, *in* Ferry, J. M., ed., Characterization of metamorphism through mineral equilibria: Washington, D.C., Mineralogical Society of America, 397 p.

Robie, R. A., Hemingway, B. S., and Fisher, J. R., 1978, Theromodynamic properties of minerals and related substances at 298.15 K and 1 Bar (10^5 Pascals) pressure and at higher temperatures: U. S. Geological Survey Bulletin 1452, 456 p.

Robie, R. A., and Waldbaum, D. R., 1968, The thermodynamic properties of minerals and related substances at 298°K (25.0°C) and one atmosphere (1,013 Bars) pressure and at higher temperatures: U. S. Geological Survey Bulletin 1259, 256 p.

Robinson, G. R., Haas, J. L., Schafer, C. M., and Haselton H. T., 1983, Thermodynamic and thermophysical properties of selected phases in the MgO-SiO_2-H_2O-CO_2, CaO-Al_2O_3-SiO_2-H_2O-CO_2, and Fe-FeO-Fe_2O_3-SiO_2 chemical systems, with special emphasis on the properties of basalts and their mineral components: U. S. Geological Survey Open File Report 83–79, 429 p.

Roozeboom, H. W. B., 1901. Die heterogenen Gleichgewichte vom Standpunkte der Phasenlehre, v. 1: Braunschweig, F. Viewig und Sohn, 218 p.

Salamon, P., Andersen, B., and Berry, S. R., 1977, Thermodynamics in finite time. II. Potentials for finite time processes: Physical Review A, v. 15, p. 2094–2102.

Saxena, S. K., and Eriksson, G., 1983, Theoretical computation of mineral assemblages in pyrolite and lherzolite: Journal of Petrology, v. 24, p. 538–555.

Saxena, S. K., and Fei, Y., 1988, Fluid mixtures in the C-H-O system at high pressure and temperature. Geochimica et Cosmochimica Acta, v. 52, p. 505–512.

Schmalzried, Von H., and Pelton, A. D., 1973, Zur geometrischen darstellung von phasengleichgewichten: Bunsengesellschaft fur Physikalische Chemie, v. 77, p. 90–94.

Schreinemakers, F. A. H., 1965, In-, mono-, and di-variant equilibria: papers by F. A. H. Schreinemakers, v. 2: University Park, The Pennsylvania State University, 325 p.

Skippen, G., 1971, Experimental data for reactions in siliceous marbles: Journal of Geology, v. 79, p. 457–481.

Skippen, G., and Trommsdorff, V., 1975, Invariant phase relations among minerals on T-X_{fluid} sections: American Journal of Science v. 275, p. 561–572.

Sundman, B., Jansson, B., and Andersson, J.-O., 1985, Thermo-Calc databank system: CALPHAD, v. 9., p. 153–186.

Thompson, A. B., 1974, Calculation of muscovite-paragonite-alkali feldspar phase relations: Contributions to Mineralogy and Petrology, v. 44, p. 173–194.

Thompson, J. B., 1954, The thermodynamic basis for the mineral facies concept: American Journal of Science, v. 253, p. 65–103.

———— 1970, Geochemical reaction and open systems: Geochimica et Cosmochimica Acta, v. 34, p. 529–551.

Thompson, J. B., and Waldbaum, D. R., 1969, Mixing properties of sanidine crystalline solutions: IV phase diagrams from equations of state: American Mineralogist, v. 54, p. 1274–1298.

Tisza, L., 1966, Generalized thermodynamics: Cambridge, Mass., M.I.T. Press, 384 p.

Trommsdorff, V., 1972, Change in T-X during metamorphism of siliceous dolomitic rocks of the Central Alps: Schweizerische Mineralogische und Petrographische Mitteilungen, v. 52, p. 1–4.

Tunell, G., 1977, Thermodynamic relations in open systems: Carnegie Institute of Washington Publication 408A, 69 p.

———— 1981, The operational basis and mathematical derivation of the Gibbs differential equation, which is the fundamental equation of chemical thermodynamics *in* Newton, R. C., Navrotsky, A., and Wood, B. J., ed., New York, Springer-Verlag, p. 1–16.

Van Zeggeren, F., and Storey, S. H., 1970, The computation of chemical equilibria: Cambridge, Cambridge Univ. Press, 333 p.

Wood, B. J., and Holloway, J. R., 1984, A thermodynamic model for subsolidus equilibria in the system CaO-MgO-Al_2O_3-SiO_2: Geochimica et Cosmochimica Acta, v. 48, p. 159–176.

Wood, B. J., and Nicholls, J., 1978, The thermodynamic properties of reciprocal solid solutions: Contributions to Mineralogy and Petrology, v. 66, p. 389–400.

Zeleznik, F. J., and Gordon, S., 1968, Calculation of complex chemical equilibria: Industrial Engineering Chemistry, v. 60, p. 27–57.

Zen, E-An, 1966a, Construction of pressure-temperature diagrams after the method of Schreinemakers—A geometric approach: U.S. Geological Survey Bulletin 1225, 56 p.

———— 1966b, Some topological relationships in multisystems of n+3 phases I. general theory; unary and binary systems: American Journal of Science, v. 264, p. 401–427.

Zhao, M., 1983, The theorem of corresponding relation between neighboring phase regions and their boundaries in phase diagrams (I): CALPHAD, v. 7, p 185–199.